

Developing fractional quantum Hall states at even-denominator fillings 1/6 and 1/8

Chengyu Wang,¹ P. T. Madathil,¹ S. K. Singh,¹ A. Gupta,¹ Y. J. Chung,¹ L. N. Pfeiffer,¹ K. W. Baldwin,¹ and M. Shayegan¹

¹*Department of Electrical and Computer Engineering,
Princeton University, Princeton, New Jersey 08544, USA*

(Dated: February 26, 2025)

In the extreme quantum limit, when the Landau level filling factor $\nu < 1$, the dominant electron-electron interaction in low-disorder two-dimensional electron systems leads to exotic many-body phases. The ground states at even-denominator $\nu = 1/2$ and $1/4$ are typically Fermi seas of composite fermions carrying two and four flux quanta, surrounded by the Jain fractional quantum Hall states (FQHSs) at odd-denominator fillings $\nu = p/(2p \pm 1)$ and $\nu = p/(4p \pm 1)$, where p is an integer. For $\nu < 1/5$, an insulating behavior, which is generally believed to signal the formation of a pinned Wigner crystal, is seen. Our experiments on ultrahigh-quality, dilute, GaAs two-dimensional electron systems reveal developing FQHSs at $\nu = p/(6p \pm 1)$ and $\nu = p/(8p \pm 1)$, manifested by magnetoresistance minima superimposed on the insulating background. In stark contrast to $\nu = 1/2$ and $1/4$, however, we observe a pronounced, sharp minimum in magnetoresistance at $\nu = 1/6$ and a somewhat weaker minimum at $\nu = 1/8$, suggesting developing FQHSs, likely stabilized by the pairing of composite fermions that carry six and eight flux quanta. Our results signal the unexpected entry, in ultrahigh-quality samples, of FQHSs at *even-denominator* fillings $1/6$ and $1/8$, which are likely to harbor non-Abelian anyon excitations.

When a two-dimensional electron system (2DES) at low temperatures is subjected to a large, perpendicular magnetic field (B), the electrons' kinetic energy is quenched as they occupy quantized, dispersionless Landau levels (LLs). The dominant electron-electron Coulomb energy leads to a variety of exotic, strongly-correlated, many-body ground states, depending on the LL filling factor $\nu = nh/eB$, where n is the 2DES density. When ν is a rational fraction, fractional quantum Hall states (FQHSs), incompressible liquid states that host quasiparticles with fractional charge and anyonic statistics, manifest as the ground states [1–5]. Of particular interest are FQHSs observed at *even-denominator* fillings of excited-state ($N=1$) LLs, e.g., at $\nu = 5/2$ [6], because they are likely to harbor non-Abelian anyon excitations [7, 8], which can be useful for topological quantum computation [9]. However, the vast majority of FQHSs are observed in the extreme quantum limit ($\nu < 1$) at *odd-denominator* fillings, and are successfully explained by Laughlin's wave function [10] and Jain's composite fermion (CF) theory [2, 11].

Another longstanding, fundamental, and important question relates to the fate of a clean 2DES at extremely small ν . It is generally believed that, for sufficiently small ν , electrons should form an ordered array, known as the Wigner crystal (WC) [12, 13]. Theorists predict a termination of the FQHSs and transition into a quantum WC at a critical ν ranging from $1/6$ to $1/11$ [10, 14–17]. On the experimental front, strong evidence for pinned WC states was reported at $\nu \lesssim 1/5$ in GaAs 2DESs [18–22]. The WC exhibits an insulating behavior because of the pinning by the ubiquitous disorder in a realistic (non-ideal) 2DES. In the highest quality samples, signatures of FQHSs were also reported in the very small filling regime,

e.g. at $\nu = 1/7$, in the form of resistance minima superimposed on the strongly insulating background [23–25]. These observations highlight the very close competition between the WC and FQHS phases.

In this work, we examine the regime of $\nu \ll 1$ in ultrahigh-quality GaAs 2DESs. We observe an unexpected emergence of new correlated states deep in the WC regime, namely *even-denominator* FQHSs at $\nu = 1/6$ and $1/8$. These states are likely non-Abelian FQHSs stabilized by the pairing of six-flux and eight-flux CFs (${}^6\text{CFs}$ and ${}^8\text{CFs}$). The presence of these large-flux CFs is also evinced by the observation of numerous odd-denominator FQHSs on the flanks of $\nu = 1/6$ and $1/8$, following the Jain sequence of ${}^6\text{CFs}$ and ${}^8\text{CFs}$.

We studied high-quality 2DESs confined to GaAs quantum wells (QWs) grown on GaAs (001) substrates by molecular beam epitaxy. They were grown following the optimization of the growth chamber vacuum integrity and the purity of the source materials [26]. We used 4×4 mm² van der Pauw geometry samples with alloyed In:Sn contacts at the four corners and side midpoints. The samples were cooled in a dilution refrigerator. We measured the longitudinal resistances (R_{xx}) using the conventional lock-in amplifier technique.

As highlighted in Fig. 1(a), on the flanks of $\nu = 1/6$, we observe a sequence of minima at $\nu = 1/5, 2/11, 3/17$, and $1/7, 2/13, 3/19$, superimposed on an extremely large and insulating R_{xx} [27]. These are the Jain-sequence FQHSs of ${}^6\text{CFs}$ [$\nu = p/(6p \pm 1)$], emanating from $\nu = 1/6$, analogous to the standard Jain-sequence FQHSs of ${}^2\text{CFs}$ and ${}^4\text{CFs}$ observed on the flanks of CF Fermi seas at $\nu = 1/2$ and $1/4$; see Fig. S4 in Supplemental Material (SM) [28] for data near $\nu = 1/2$ and $1/4$. Our observation is consistent with recent calculations which indicate that, in the

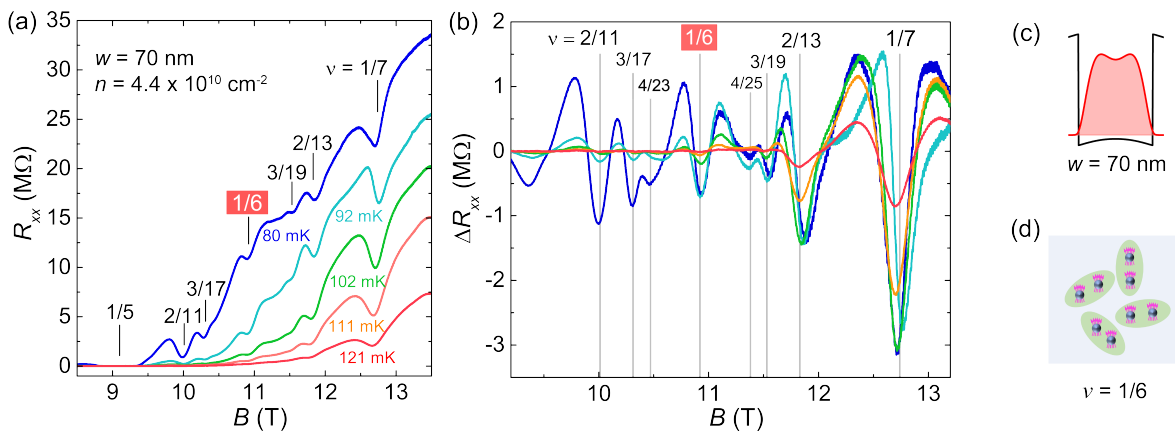


FIG. 1. (a) Longitudinal resistance (R_{xx}) vs perpendicular magnetic field (B) traces for our ultrahigh-mobility 2DES in the extremely small filling regime ($1/5 > \nu > 1/7$), measured at different temperatures [27]. The 2DES is confined to a 70-nm-wide QW, and has a density of $4.4 \times 10^{10} \text{ cm}^{-2}$ and a record mobility of $22 \times 10^6 \text{ cm}^2/\text{Vs}$ at this density. The magnetic field positions of several LL fillings are marked. Our data exhibit numerous local minima in R_{xx} at odd-denominator fillings $1/5$, $2/11$, $3/17$, $1/7$, $2/13$, and $3/19$. These fillings correspond to the Jain-sequence states of six-flux CFs (${}^6\text{CF}$). Remarkably, we also observe a local minimum in R_{xx} at the *even-denominator* filling $\nu=1/6$, suggesting a developing FQHS. (b) ΔR_{xx} vs B traces for the same set of data, where ΔR_{xx} is the resistance after subtracting the increasing, smooth background [28]. (c) Self-consistent charge distribution (red) and potential (black) for the 2DES. (d) A possible origin of the $1/6$ FQHS: Each electron captures six flux quanta to turn into a ${}^6\text{CF}$. Then ${}^6\text{CF}$ s undergo a pairing instability and condense into a FQHS.

low-disorder limit, Jain-sequence FQHSs of ${}^6\text{CF}$ s should prevail at $\nu=1/7$ and $2/13$ [17]. The appearances of the very-high-order FQHSs near $\nu=1/2$ and $1/4$, and the rarely observed FQHSs near $\nu=1/6$ [23–25], collectively demonstrate the exceptionally high quality of our 2DES, specially at such a low density ($n=4.4$, in units of 10^{10} cm^{-2} , which we use throughout the paper).

Our main finding is the pronounced, sharp minimum in R_{xx} at the *even-denominator* filling $\nu=1/6$. As we illustrate below, the characteristics of this minimum are very similar to those of the nearby, emerging, odd-denominator FQHSs. Our data signal a developing even-denominator FQHS at $\nu=1/6$, likely stabilized by the pairing of ${}^6\text{CF}$ s.

Figure 1(a) also shows high-field R_{xx} vs B traces at different temperatures. As T increases from 80 to 121 mK, R_{xx} at $\nu < 1/5$ decreases by more than an order of magnitude. Meanwhile, R_{xx} minima at $\nu=1/6$ and $\nu=p/(6p\pm 1)$ gradually weaken and eventually turn into inflection points [28, 39]. To highlight FQHS features, in Fig. 1(b), we present ΔR_{xx} vs B traces, with ΔR_{xx} representing resistance after subtracting the smooth background; see Section I of SM for details [28]. We observe sharp ΔR_{xx} minima at $\nu=p/(6p\pm 1)$ for $p=1, 2, 3, 4$, and at $\nu=1/6$. The $\nu=p/(6p\pm 1)$ minima are weaker for larger p and weaken with increasing T , consistent with standard Jain-sequence FQHSs. The $\nu=1/6$ minimum is sharp and exhibits similar temperature dependence to those at Jain-sequence fillings, signaling a developing FQHS at $\nu=1/6$.

We note that with decreasing temperature, instead of

approaching zero, R_{xx} at $\nu=1/6$ and $p/(6p\pm 1)$ increases. This is because an insulating behavior, which is a manifestation of a pinned WC [18–22], is dominant in the whole range of $\nu < 1/5$. Our observation signals a close competition between the FQHSs and WC states. More specifically, the energies of WC and FQHSs are so close that FQHSs only win in a very narrow range of ν [17]. Therefore, in a realistic 2DES, a small local variation of filling factor caused by a minuscule density inhomogeneity or disorder can lead to the formation of WC domains and prevent the percolation of the FQH liquid [40]. Our data are reminiscent of what was historically observed at $\nu=1/5$ in GaAs 2DESs [19, 20, 37, 38, 41, 42]. Initially, in modest-quality samples, only an R_{xx} minimum that rose with decreasing temperature was seen because of the significant amount of disorder [41, 42]. With improved sample quality, percolation of the FQH liquid was eventually achieved, exhibiting a vanishing R_{xx} accompanied by a quantized Hall plateau, firmly establishing that the ground state at $\nu=1/5$ is a FQHS [19, 37, 38].

We measured a second sample from the same wafer [43]. Figure 2(a) shows the R_{xx} vs $1/\nu$ traces measured at $T \simeq 80$ mK with n ranging from 2.77 to 5.10, while maintaining symmetric charge distribution. We observe a clear inflection point at $\nu=1/6$. It becomes weaker at lower densities [44]. In addition, well-defined R_{xx} minima are observed at $\nu=2/11$ in the whole range of n , and at $\nu=1/7$ in the lower density traces where we could reach $\nu=1/7$ with our magnet. Figure 2(b) displays a color-scale plot of ΔR_{xx} as a function of $1/\nu$ and n . Distinct ΔR_{xx} minima are observed at $\nu=2/11, 3/17, 3/19, 1/6,$

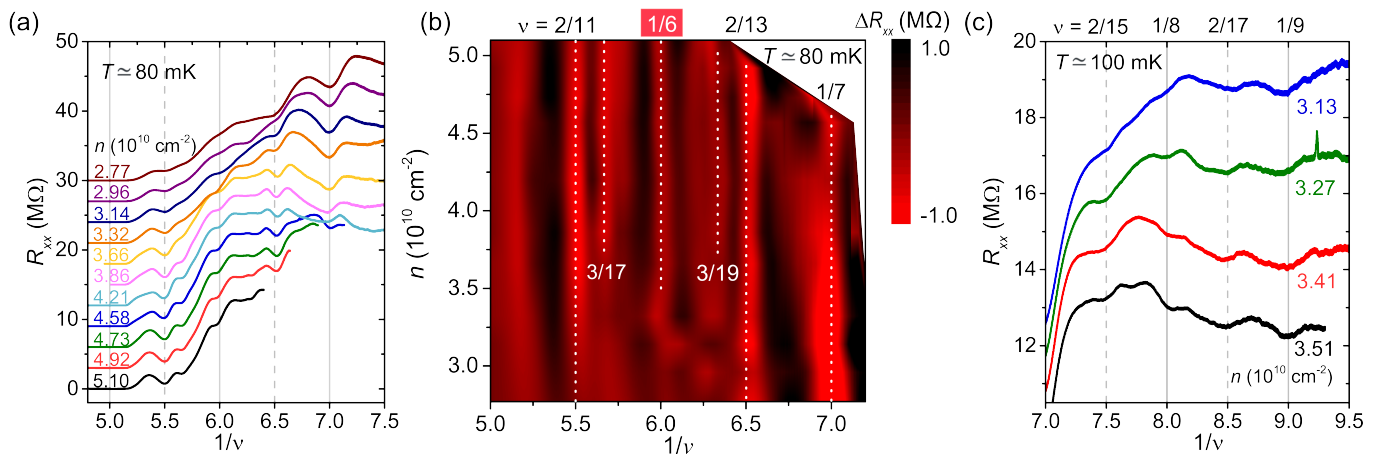


FIG. 2. **Density dependence.** (a) R_{xx} vs $1/\nu$ traces measured at $T \simeq 80 \text{ mK}$ for different densities n . Each trace is vertically shifted by $3 \text{ M}\Omega$ for clarity. n is tuned by symmetrically gating the 2DES from both the top and bottom. (b) Color-scale plot of ΔR_{xx} as a function of $1/\nu$ and n . Several fillings are marked by white dotted lines. (c) R_{xx} vs $1/\nu$ traces measured at $T \simeq 100 \text{ mK}$ and at very small ν . R_{xx} minima are observed at $\nu = 1/9, 2/17, 1/8, \text{ and } 2/15$.

$2/13$, and $1/7$, with their $1/\nu$ positions remaining consistent across different n , indicating that the signatures of the even-denominator FQHS at $\nu = 1/6$, as well as the high-order Jain-sequence FQHSs at $\nu = p/(6p \pm 1)$, are intrinsic to our ultrahigh-quality 2DES.

Figure 2(c) data show the fate of the FQHSs at yet smaller ν . Here we observe R_{xx} minima at odd-denominator $\nu = 1/9, 2/17, \text{ and } 2/15$. Hints of developing FQHSs were previously reported at $\nu = 1/9$ by optical and transport measurements [24, 45]. Recent calculations also suggest that the ground state at $\nu = 1/9$ is likely a FQHS [17]. Our data revealing R_{xx} minima at fixed fillings over a range of densities provide strong evidence for the existence of FQHSs at $\nu = p/(8p \pm 1)$, namely at $\nu = 1/9, 2/17, \text{ and } 2/15$ [46]. Furthermore, the traces also exhibit an R_{xx} minimum (or an inflection point) at the *even-denominator* filling $\nu = 1/8$. The qualitative resemblance of the data near $\nu = 1/8$ in Fig. 2(c) to Fig. 2(a) data suggests that the physics for ${}^6\text{CFs}$ for $1/7 < \nu < 1/5$ can be extended to ${}^8\text{CFs}$ for $1/9 < \nu < 1/7$.

The signatures of the $\nu = 1/6$ FQHS are not specific to one wafer. In Fig. 3 we present data for another ultrahigh-quality GaAs 2DES from a different wafer with a higher density of 7.1 and a narrower QW width of 58.5 nm . We find a clear, sharp R_{xx} minimum at $\nu = 1/6$ at 108 mK [47], and an inflection point at a slightly higher temperature of 116 mK .

One potential competitive ground state at $\nu = 1/6$ is a metallic Fermi sea of ${}^6\text{CFs}$ at zero effective magnetic field. However, several observations suggest that the R_{xx} minimum we observe at $\nu = 1/6$ is not indicative of a ${}^6\text{CF}$ Fermi sea: (i) At $\nu = 1/2$, where a Fermi sea of ${}^2\text{CFs}$ is well established, typically a smooth and broad minimum in R_{xx} is observed; see, e.g., Figs. S4 and S5 in SM [28]. In contrast, the R_{xx} minimum at $\nu = 1/6$ is sharp; see

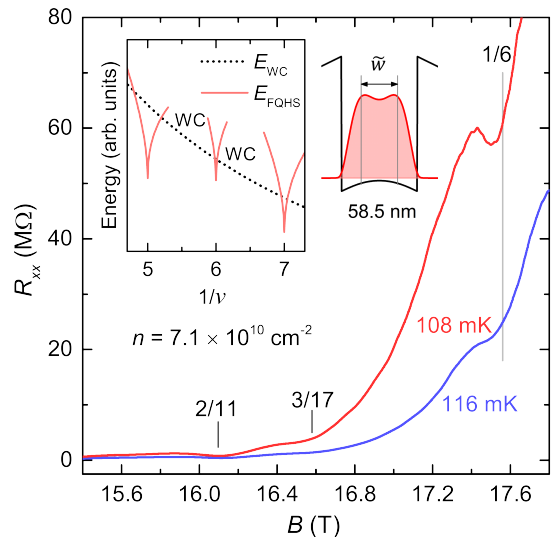


FIG. 3. **Data for a different sample.** R_{xx} vs B traces for a sample with a density of $7.1 \times 10^{10} \text{ cm}^{-2}$. Left inset: Schematic diagram showing the energies of WC and FQHS vs $1/\nu$, indicating the possibility of a downward cusp in energy at $1/\nu = 6$, similar to cusps at $1/\nu = 5$ and 7 . Right inset: Self-consistent charge distribution (red) and potential (black) for the 2DES confined to a 58.5 nm -wide QW; \tilde{w} denotes the electron layer thickness (see text).

Figs. 1 and 3, and also the sharp peak in $d^2 R_{xx}/dB^2$ [Fig. S2(b)]. The sharp R_{xx} minimum observed in the WC regime at $\nu = 1/6$ indicates that the $\nu = 1/6$ state is flanked by WC states. This strongly favors the interpretation of FQHS over ${}^6\text{CF}$ Fermi sea: The energies of FQHSs show downward cusps as a function of ν , and can dip below the WC energy (see Fig. 3 left inset, and also

TABLE I. **Sample parameters**

Sample	density (10^{10} cm^{-2})	mobility ($10^6 \text{ cm}^2/\text{Vs}$)	QW width (nm)	\tilde{w}/l_B (at $\nu=1/6$)	$\Delta_{\text{SAS}}/E_{\text{Coul}}$ (at $\nu=1/6$)	strength of $\nu=1/6$ FQHS feature
A	4.4	22	70	4.3	0.13	Strong
B	7.1	25	58.5	4.6	0.15	Strong
C	4.3	16	50	2.7	0.33	Weak
D	4.5	17	40	2.2	0.52	Weak
E	4.3	10	30	1.7	0.93	Absent

see Fig. 9 in Ref. [48]) so that the WC could be reentrant on the flanks of a FQHS [17, 19, 33]. On the other hand, the energies of both CF Fermi sea and WC states are smooth functions of ν , and thus one would expect only a single transition between these two states. (ii) The R_{xx} minimum at $\nu=1/6$ and its temperature dependence closely resemble those at Jain-sequence, odd-denominator fillings, such as $\nu=1/7$ (see Fig. 1 and also Fig. S6 in SM [28, 39]), challenging the metallic ${}^6\text{CF}$ Fermi sea interpretation. (iii) A broad R_{xx} minimum is not a universal feature for a CF Fermi sea, and is indeed generally absent at $\nu=1/4$ when there is a competing insulating phase or rising background resistance [49]; also see SM [28]. It is also worth noting that the observation of Jain-sequence FQHSs does not necessarily indicate the presence of a CF Fermi sea. Indeed, a FQHS at $\nu=1/2$ flanked by numerous Jain-sequence FQHSs is well established in 2DESs confined to wide GaAs QWs [50, 51, 53–57]. We emphasize that, while we believe our data favor the presence of a developing FQHS at $\nu=1/6$, taking the R_{xx} minimum as evidence for a ${}^6\text{CF}$ Fermi sea at $1/6$ is also novel as there has been no experimental or theoretical evidence for such a phase deep in the low-filling, insulating, WC regime.

The emergence of even-denominator FQHSs at $\nu=1/6$ and $1/8$ is unexpected. These states have not been reported in any 2D carrier system, or predicted by existing theories. One might wonder if these new enigmatic states share a common origin with two other even-denominator FQHSs, namely those at $\nu=1/2$ and $1/4$, observed in the lowest LL in wide QWs under special circumstances [50–57]. The origin of these states has been a subject of debate [58]; however, recent experiments [55–57] and theories [59–61] indicate they are likely single-component, non-Abelian states arising from a pairing instability of CFs. To examine this possibility and investigate the role of QW width on the $1/6$ FQHS, we studied several samples with similar densities $n=4.4, 4.3, 4.5$ and 4.3 , but different QW widths of 70, 50, 40, and 30 nm, respectively. Below we summarize our findings; for details, see Sec. IV in SM [28].

Table I contains the relevant parameters for our samples. One parameter is the effective electron layer thickness (\tilde{w}), normalized to the magnetic length $l_B = \sqrt{\hbar/eB}$; \tilde{w} is typically defined as twice the standard devi-

ation of the calculated charge distribution from its center; see Fig. 3 inset for an example. Another parameter is the symmetric-to-antisymmetric subband separation (Δ_{SAS}) normalized to the Coulomb energy, $E_{\text{Coul}} = e^2/(4\pi\epsilon l_B)$. For 2DESs confined to QWs, in the extreme quantum limit ($\nu < 1$), although only one LL that originates from the symmetric subband is partially occupied, the proximity of the antisymmetric subband can potentially modify the electron-electron interaction in the lowest LL when $\Delta_{\text{SAS}}/E_{\text{Coul}} \ll 1$. As seen in Table I, we observe the strongest $\nu=1/6$ FQHS in samples A and B where \tilde{w}/l_B is large ($\gtrsim 4$) and $\Delta_{\text{SAS}}/E_{\text{Coul}}$ is small ($\lesssim 0.2$), suggesting that the $\nu=1/6$ FQHS is stabilized by the large layer thickness and proximity of the antisymmetric subband.

While the $1/2$ and $1/4$ FQHSs are also seen at large \tilde{w}/l_B and reasonably small $\Delta_{\text{SAS}}/E_{\text{Coul}}$, the $1/6$ data pose several notable quantitative and qualitative differences. First, the parameters for the samples where we observe the strong $\nu=1/6$ minima are different compared to those where the $1/2$ and $1/4$ FQHSs are seen. This is visually exhibited in “phase diagrams” for the stability of the $\nu=1/2$ FQHS in wide GaAs QWs shown in Fig. S9 in SM [28]. Second, the $1/2$ and $1/4$ FQHSs are observed only in samples with *bilayer* charge distributions [50–57], but in our samples the charge distribution is single-layer, albeit thick [see Fig. 1(c) and Fig. 3 inset]. Third, the $1/2$ and $1/4$ FQHSs in wide QWs become weaker and disappear when the charge distribution is made asymmetric [51, 53, 62]. In contrast, the developing $1/6$ FQHS in our sample is robust against asymmetry (see Figs. S10 and S11 [28]). Fourth, at a fixed QW width, by increasing n , or equivalently \tilde{w}/l_B , the ground state at $\nu=1/2$ in wide QWs starts as a compressible Fermi sea, transitions to an incompressible FQHS, and eventually turns into an insulating phase [51, 54, 62]. At $\nu=1/6$, however, the 2DES is deep in the insulating regime, and a developing FQHS emerges when \tilde{w}/l_B becomes large.

It is worth reiterating that, while the origin of the $1/2$ FQHS in wide QWs is not entirely clear, recent experiments [55–57] and theories [59, 61] point to a single-component, non-Abelian, Pfaffian-like state stabilized by a p -wave pairing of ${}^2\text{CFs}$. Similarly, the $1/4$ FQHS has been interpreted as a single-component, non-Abelian FQHS stabilized by f -wave pairing of ${}^4\text{CFs}$ [60, 61]. Despite the differences enumerated in the pre-

vious paragraph between the parameters of our samples and those which show the $1/2$ and $1/4$ FQHSs, we suggest that the developing $1/6$ FQHS we report here is also single-component and non-Abelian, and is stabilized by a pairing of ${}^6\text{CFs}$ [see Fig. 1(d)]. An alternative, two-component ground state, such as the Halperin-Laughlin Ψ_{993} state [63], is extremely unlikely to be the ground state, given the single-layer-like charge distribution in our samples and the persistence of the $1/6 R_{xx}$ minimum as we make the charge distribution significantly asymmetric. Consistent with our conjecture that the $1/6$ FQHS we are observing has a one-component origin, preliminary theoretical calculations indeed suggest that this state likely emerges from an f -wave pairing of ${}^6\text{CFs}$ and hosts non-Abelian quasiparticles [64]. We hope, of course, that our results will stimulate future theoretical calculations to shed more light on the origin of the FQHSs at $\nu = 1/6$ (and $1/8$).

Acknowledgments — We acknowledge support by the National Science Foundation (NSF) Grants No. DMR 2104771 and No. ECCS 1906253) for measurements, the U.S. Department of Energy (DOE) Basic Energy Sciences Grant No. DEFG02-00-ER45841) for sample characterization, the Eric and Wendy Schmidt Transformative Technology Fund, and the Gordon and Betty Moore Foundation’s EPiQS Initiative (Grant No. GBMF9615.01 to L.N.P.) for sample fabrication. Our measurements were partly performed at the National High Magnetic Field Laboratory (NHMFL), which is supported by the NSF Cooperative Agreement No. DMR 2128556, by the State of Florida, and by the DOE. This research was funded in part by QuantEmX grant from Institute for Complex Adaptive Matter and the Gordon and Betty Moore Foundation through Grant GBMF9616 to C. W., A. G., P. T. M., and S. K. S. We thank A. Bangura, G. Jones, R. Nowell and T. Murphy at NHMFL for technical assistance, and Ajit C. Balram and Jainendra K. Jain for illuminating discussions.

[1] D. C. Tsui, H. L. Stormer, and A. C. Gossard, Two-Dimensional Magnetotransport in the Extreme Quantum Limit, *Phys. Rev. Lett.* **48**, 1559 (1982).
 [2] J. K. Jain, *Composite fermions*, (Cambridge University Press, Cambridge, England, 2007).
 [3] *Fractional Quantum Hall Effects: New Developments*, edited by B. I. Halperin and J. K. Jain (World Scientific, Singapore, 2020).
 [4] J. Nakamura, S. Liang, G. C. Gardner, and M. J. Manfra, Direct observation of anyonic braiding statistics, *Nat. Phys.* **16**, 931 (2020).
 [5] H. Bartolomei, M. Kumar, R. Bisognin, A. Marguerite, J.-M. Berroir, E. Bocquillon, B. Plaças, A. Cavanna, Q. Dong, U. Gennser, Y. Jin, and G. Fève, Fractional statistics in anyon collisions, *Science* **368**, 173 (2020).
 [6] R. Willett, J. P. Eisenstein, H. L. Störmer, D. C. Tsui, A.

C. Gossard, and J. H. English, Observation of an even-denominator quantum number in the fractional quantum Hall effect, *Phys. Rev. Lett.* **59**, 1776 (1987).
 [7] M. Banerjee, M. Heiblum, V. Umansky, D. E. Feldman, Y. Oreg, and A. Stern, Observation of half-integer thermal Hall conductance, *Nature* **559**, 205 (2018).
 [8] R. L. Willett, K. Shtengel, C. Nayak, L. N. Pfeiffer, Y. J. Chung, M. L. Peabody, K. W. Baldwin, and K. W. West, Interference Measurements of Non-Abelian $e/4$ & Abelian $e/2$ Quasiparticle Braiding, *Phys. Rev. X* **13**, 011028 (2023).
 [9] Chetan Nayak, Steven H. Simon, Ady Stern, Michael Freedman, and Sankar Das Sarma, Non-Abelian anyons and topological quantum computation, *Rev. Mod. Phys.* **80**, 1083 (2008).
 [10] R. B. Laughlin, Anomalous Quantum Hall Effect: An Incompressible Quantum Fluid with Fractionally Charged Excitations, *Phys. Rev. Lett.* **50**, 1395 (1983).
 [11] J. K. Jain, Composite-fermion approach for the fractional quantum Hall effect, *Phys. Rev. Lett.* **63**, 199 (1989).
 [12] E. Wigner, On the Interaction of Electrons in Metals, *Phys. Rev.* **46**, 1002 (1934).
 [13] M. Shayegan, Wigner crystals in flat band 2D electron systems, *Nat. Rev. Phys.* **4**, 212 (2022).
 [14] Pui K. Lam and S. M. Girvin, Liquid-solid transition and the fractional quantum-Hall effect, *Phys. Rev. B* **30**, 473 (1984).
 [15] Keivan Esfarjani and S. T. Chui, Solidification of the two-dimensional electron gas in high magnetic fields, *Phys. Rev. B* **42**, 10758 (1990).
 [16] Kun Yang, F. D. M. Haldane, and E. H. Rezayi, Wigner crystals in the lowest Landau level at low-filling factors, *Phys. Rev. B* **64**, 081301 (2001).
 [17] Zheng-Wei Zuo, Ajit C. Balram, Songyang Pu, Jianyun Zhao, Thierry Jolicoeur, A. Wójs, and J. K. Jain, Interplay between fractional quantum Hall liquid and crystal phases at low filling, *Phys. Rev. B* **102**, 075307 (2020).
 [18] E. Y. Andrei, G. Deville, D. C. Glatli, F. I. B. Williams, E. Paris, and B. Etienne, Observation of a Magnetically Induced Wigner Solid, *Phys. Rev. Lett.* **60**, 2765 (1988).
 [19] H. W. Jiang, R. L. Willett, H. L. Stormer, D. C. Tsui, L. N. Pfeiffer, and K. W. West, Quantum liquid versus electron solid around $\nu = 1/5$ Landau-level filling, *Phys. Rev. Lett.* **65**, 633 (1990).
 [20] V. J. Goldman, M Santos, M Shayegan, and J. E. Cunningham, Evidence for two-dimensional quantum Wigner crystal, *Phys. Rev. Lett.* **65**, 2189 (1990).
 [21] Y. P. Chen, G. Sambandamurthy, Z. H. Wang, R. M. Lewis, L. W. Engel, D. C. Tsui, P. D. Ye, L. N. Pfeiffer, and K. W. West, Melting of a 2D quantum electron solid in high magnetic field, *Nat. Phys.* **2**, 452 (2006).
 [22] H. Deng, Y. Liu, I. Jo, L. N. Pfeiffer, K. W. West, K. W. Baldwin, and M. Shayegan, Commensurability Oscillations of Composite Fermions Induced by the Periodic Potential of a Wigner Crystal, *Phys. Rev. Lett.* **117**, 096601 (2016).
 [23] V. J. Goldman, M. Shayegan, and D. C. Tsui, Evidence for the Fractional Quantum Hall State at $\nu = 1/7$, *Phys. Rev. Lett.* **61**, 881 (1988).
 [24] W. Pan, H. L. Stormer, D. C. Tsui, L. N. Pfeiffer, K. W. Baldwin, K. W. West, Transition from an electron solid to the sequence of fractional quantum Hall states at very low Landau level filling factor, *Phys. Rev. Lett.* **88**, 176802 (2002).

- [25] Yoon Jang Chung, D. Graf, L. W. Engel, K. A. Villegas Rosales, P. T. Madathil, K. W. Baldwin, K. W. West, L. N. Pfeiffer, and M. Shayegan, Correlated States of 2D Electrons near the Landau Level Filling $\nu = 1/7$, *Phys. Rev. Lett.* **128**, 026802 (2022).
- [26] Yoon Jang Chung, K. A. Villegas Rosales, K. W. Baldwin, P. T. Madathil, K. W. West, M. Shayegan and L. N. Pfeiffer, Ultra-high-quality two-dimensional electron systems, *Nat. Mater.* **20**, 632-637 (2021).
- [27] In Fig. 1(a), to measure high R_{xx} ($\sim M\Omega$), a small driving ac current (0.2 nA) with low frequency (0.05 Hz) was used to avoid heating and nonlinear effects, and to maximize the in-phase (resistive) component of the signal.
- [28] See Supplemental Material for additional magnetotransport data and discussions, which includes Refs. [29–38].
- [29] R. L. Willett, R. R. Ruel, K. W. West, and L. N. Pfeiffer, Experimental demonstration of a Fermi surface at one-half filling of the lowest Landau level, *Phys. Rev. Lett.* **71**, 3846 (1993).
- [30] W. Kang, H. L. Stormer, L. N. Pfeiffer, K. W. Baldwin, and K. W. West, How real are composite fermions?, *Phys. Rev. Lett.* **71**, 3850 (1993).
- [31] D. Kamburov, Yang Liu, M. A. Mueed, M. Shayegan, L. N. Pfeiffer, K. W. West, and K. W. Baldwin, What Determines the Fermi Wave Vector of Composite Fermions?, *Phys. Rev. Lett.* **113**, 196801 (2014).
- [32] Md. Shafayat Hossain, Meng K. Ma, M. A. Mueed, D. Kamburov, L. N. Pfeiffer, K. W. West, K. W. Baldwin, R. Winkler, and M. Shayegan, Geometric resonance of four-flux composite fermions, *Phys. Rev. B* **100**, 041112(R) (2019).
- [33] Alexander C. Archer, Kwon Park, and Jainendra K. Jain, Competing Crystal Phases in the Lowest Landau Level, *Phys. Rev. Lett.* **111**, 146804 (2013).
- [34] Alexander C. Archer and Jainendra K. Jain, Quantum bubble defects in the lowest-Landau-level crystal, *Phys. Rev. B* **90**, 201309 (2014).
- [35] P. T. Madathil, C. Wang, S. K. Singh, A. Gupta, K. A. Villegas Rosales, Y. J. Chung, K. W. West, K. W. Baldwin, L. N. Pfeiffer, L. W. Engel, and M. Shayegan, Signatures of Correlated Defects in an Ultraclean Wigner Crystal in the Extreme Quantum Limit, *Phys. Rev. Lett.* **132**, 096502 (2024).
- [36] P. T. Madathil, K. A. Villegas Rosales, Y. J. Chung, K. W. West, K. W. Baldwin, L. N. Pfeiffer, L. W. Engel, and M. Shayegan, Moving Crystal Phases of a Quantum Wigner Solid in an Ultra-High-Quality 2D Electron System, *Phys. Rev. Lett.* **131**, 236501 (2023).
- [37] V. J. Goldman, J. K. Wang, B. Su, and M. Shayegan, Universality of the Hall effect in a magnetic-field-localized two-dimensional electron system, *Phys. Rev. Lett.* **70**, 647 (1993).
- [38] T. Sajoto, Y. P. Li, L. W. Engel, D. C. Tsui, and M. Shayegan, Hall resistance of the reentrant insulating phase around the $1/5$ fractional quantum Hall liquid, *Phys. Rev. Lett.* **70**, 2321 (1993).
- [39] Activation energy (E_A) data deduced from the relation $R_{xx} \propto eE_A/2kT$ as a function of B also reveal clear minima at $\nu = 1/7$, $2/11$, and $1/6$, where signatures of developing FQHSs are observed in the R_{xx} vs B data in Fig. 1(a). Similar minima in E_A were reported in modest quality GaAs 2DESs at $\nu = 1/5$ [42] and very recently in ultrahigh-quality GaAs 2DESs at $\nu = 1/7$ [25], and were interpreted as precursors to developing FQHSs. The observation of an E_A minimum at $\nu = 1/6$ therefore supports the notion that the ground state at this filling is a FQHS. See Fig. S6 in SM [28] for details.
- [40] In our samples, the extremely high values of R_{xx} ($\sim M\Omega$) preclude us from measuring the Hall resistance (R_H) accurately at small fillings $\nu < 1/5$; see SM (Section VII, Figs. S12-14) for Hall data and a detailed discussion [28]. The very large R_{xx}/R_H causes significant mixing of R_{xx} in measurements of R_H . This is a well-known problem for small ν regime where an insulating behavior is dominant [23, 25, 37, 38].
- [41] E. E. Mendez, M. Heiblum, L. L. Chang, and L. Esaki, High-magnetic-field transport in a dilute two-dimensional electron gas, *Phys. Rev. B* **28**, 4886(R) (1983).
- [42] R. L. Willett, H. L. Stormer, D. C. Tsui, L. N. Pfeiffer, K. W. West, and K. W. Baldwin, Termination of the series of fractional quantum Hall states at small filling factors, *Phys. Rev. B* **38**, 7881(R) (1988).
- [43] This sample was fitted with front and back gates, allowing us to vary the density while also tuning the charge distribution symmetry in the GaAs QW.
- [44] We note that all the FQHS features in Fig. 2(a) are somewhat weaker than in Fig. 1(a). We attribute this to the lower 2DES quality of the gated sample because of the deposition of the metal front gate on the top surface.
- [45] H. Buhmann, W. Joss, K. von Klitzing, I. V. Kukushkin, G. Martinez, A. S. Plaut, K. Ploog, and V. B. Timofeev, Magneto-optical evidence for fractional quantum Hall states down to filling factor $1/9$, *Phys. Rev. Lett.* **65** 1056 (1990).
- [46] It is worth remarking that the magneto-resistance traces in Figs. 2(a) and 2(c) exhibit a saturating behavior at the smallest fillings. This is similar to the data of Ref. [24], and its origin remains unknown.
- [47] We note that the B position of the $\nu = 1/6$ R_{xx} minimum in Fig. 3 is slightly lower compared to the expected value. This deviation ($\sim 0.3\%$) is minor and the proximity of the minimum to $\nu = 1/6$ allows us to exclude it from high-order, odd-denominator, Jain-sequence FQHSs at $\nu = p/(6p - 1)$, e.g., at $\nu = 4/23$ ($B = 16.8$ T).
- [48] M. Shayegan, Flatland Electrons in High Magnetic Fields, in *High Magnetic Fields: Science and Technology*, edited by F. Herlach and N. Miura (World Scientific, Singapore, 2006), Vol. 3, pp. 31–60; arXiv:cond-mat/0505520.
- [49] W. Pan, H. L. Stormer, D. C. Tsui, L. N. Pfeiffer, K. W. Baldwin, and K. W. West, Effective mass of the four-flux composite fermion at $\nu = 1/4$, *Phys. Rev. B* **61**, R5101(R) (2000).
- [50] Y. W. Suen, L. W. Engel, M. B. Santos, M. Shayegan, and D. C. Tsui, Observation of a $\nu = 1/2$ fractional quantum Hall state in a double-layer electron system, *Phys. Rev. Lett.* **68**, 1379 (1992).
- [51] Y. W. Suen, H. C. Manoharan, X. Ying, M. B. Santos, and M. Shayegan, Origin of the $\nu = 1/2$ fractional quantum Hall state in wide single quantum wells, *Phys. Rev. Lett.* **72**, 3405 (1994).
- [52] D. R. Luhman, W. Pan, D. C. Tsui, L. N. Pfeiffer, K. W. Baldwin, and K. W. West, Observation of a Fractional Quantum Hall State at $\nu = 1/4$ in a Wide GaAs Quantum Well, *Phys. Rev. Lett.* **101**, 266804 (2008).
- [53] J. Shabani, T. Gokmen, and M. Shayegan, Correlated

- States of Electrons in Wide Quantum Wells at Low Fillings: The Role of Charge Distribution Symmetry, *Phys. Rev. Lett.* **103**, 046805 (2009).
- [54] J. Shabani, Yang Liu, M. Shayegan, L. N. Pfeiffer, K. W. West, and K. W. Baldwin, Phase diagrams for the stability of the $\nu = 1/2$ fractional quantum Hall effect in electron systems confined to symmetric, wide GaAs quantum wells, *Phys. Rev. B* **88**, 245413 (2013).
- [55] M. A. Mueed, D. Kamburov, S. Hasdemir, M. Shayegan, L. N. Pfeiffer, K. W. West, and K. W. Baldwin, Geometric Resonance of Composite Fermions Near the $\nu = 1/2$ Fractional Quantum Hall State, *Phys. Rev. Lett.* **114**, 236406 (2015).
- [56] M. A. Mueed, D. Kamburov, L. N. Pfeiffer, K. W. West, K. W. Baldwin, and M. Shayegan, Geometric Resonance of Composite Fermions near Bilayer Quantum Hall States, *Phys. Rev. Lett.* **117**, 246801 (2016).
- [57] S. K. Singh, C. Wang, C. T. Tai, C. S. Calhoun, K. A. Villegas Rosales, P. T. Madathil, A. Gupta, K. W. Baldwin, L. N. Pfeiffer, M. Shayegan, Topological phase transition between Jain states and daughter states of the $\nu = 1/2$ fractional quantum Hall state *Nat. Phys.* **20**, 1247 (2024).
- [58] Michael R. Peterson and S. Das Sarma, Quantum Hall phase diagram of half-filled bilayers in the lowest and the second orbital Landau levels: Abelian versus non-Abelian incompressible fractional quantum Hall states, *Phys. Rev. B* **81**, 165304 (2010).
- [59] W. Zhu, Zhao Liu, F. D. M. Haldane, and D. N. Sheng, Fractional quantum Hall bilayers at half filling: Tunneling-driven non-Abelian phase, *Phys. Rev. B* **94**, 245147 (2016).
- [60] W. N. Faugno, Ajit C. Balram, Maissam Barkeshli, and J. K. Jain, Prediction of a Non-Abelian Fractional Quantum Hall State with f-Wave Pairing of Composite Fermions in Wide Quantum Wells, *Phys. Rev. Lett.* **123**, 016802 (2019).
- [61] Anirban Sharma, Ajit C. Balram, and J. K. Jain, Composite-fermion pairing at half and quarter filled lowest Landau level, *Phys. Rev. B* **109**, 035306 (2024).
- [62] H. C. Manoharan, Y. W. Suen, M. B. Santos, and M. Shayegan, Evidence for a Bilayer Quantum Wigner Solid, *Phys. Rev. Lett.* **77**, 1813 (1996).
- [63] A. H. MacDonald, The fractional Hall effect in multi-component systems, *Surface Science* **229**, 1 (1990).
- [64] A. Sharma, A. C. Balram, and J. K. Jain, unpublished.

**Supplemental Material to “Developing fractional quantum Hall
states at even-denominator fillings $1/6$ and $1/8$ ”**

Chengyu Wang,¹ P. T. Madathil,¹ S. K. Singh,¹ A. Gupta,¹ Y.
J. Chung,¹ L. N. Pfeiffer,¹ K. W. Baldwin,¹ and M. Shayegan¹

¹*Department of Electrical and Computer Engineering,
Princeton University, Princeton, New Jersey 08544, USA*

(Dated: November 13, 2024)

I. TWO METHODS OF EXTRACTING FRACTIONAL QUANTUM HALL STATE FEATURES FROM HIGHLY INSULATING LONGITUDINAL RESISTANCE

In order to better visualize the fractional quantum Hall state (FQHS) features in R_{xx} amidst the dominant insulating behavior caused by the competing Wigner crystal (WC) states, we extract the oscillatory component (ΔR_{xx}) of the R_{xx} data. Here ΔR_{xx} is defined as the resistance after subtracting the smooth background. Figures S1(a-h) display the raw R_{xx} traces (black) and their corresponding smooth backgrounds (red) obtained using second-order Savitzky-Golay smoothing with a window size of 1.5 T. This window size captures the main trend of the slowly varying part of R_{xx} without introducing artificial features. To ensure consistency across different densities, the window sizes we use for obtaining ΔR_{xx} in Fig. 2(b) of the main text are scaled according to the density. Figure S1(i) shows a color-scale plot of ΔR_{xx} as a function of B and T . In Fig. S1(j) we show the same set of data by plotting ΔR_{xx} vs B traces at different temperatures. Clear minima are observed at $\nu = 2/11, 3/17, 4/23, 1/6, 4/25, 3/19, 2/13,$ and $1/7$, suggesting the emergence of FQHSs at these fillings. The data reveal that the odd-denominator FQHS features become less robust as the filling factor approaches $\nu = 1/6$, consistent with what is generally observed for standard Jain-sequence FQHSs. Furthermore, the ΔR_{xx} minimum at $\nu = 1/6$ is sharp, and shows a strong temperature dependence. This is very similar to the ΔR_{xx} minima at odd-denominator fillings on the flanks of $\nu = 1/6$, but very different compared to the smooth, broad R_{xx} minimum at $\nu = 1/2$ which is rather insensitive to small temperature changes.

Another effective method to extract FQHS features from highly insulating R_{xx} data is to calculate the second derivative, $d^2 R_{xx}/dB^2$. A developing FQHS manifests itself as a sharp, maximal curvature in R_{xx} , and therefore exhibits a sharp peak in $d^2 R_{xx}/dB^2$. In Fig. S2, we compare the color-scale plot of $d^2 R_{xx}/dB^2$ as a function of B and T [panel (b)] to data in Fig. S1(i) [replotted as panel (a) of Fig. S2]. Both methods reveal sharp FQHS features at $\nu = 1/6$ and odd-denominator, Jain-sequence fillings $\nu = p/(6p \pm 1)$. As another example of the similarity between ΔR_{xx} and $d^2 R_{xx}/dB^2$, in Fig. S3 we show color-scale plots of ΔR_{xx} [panel (a)] and $d^2 R_{xx}/dB^2$ [panel (b)] as a function of $1/\nu$ and n .

II. MAGNETO-TRANSPORT DATA NEAR LANDAU LEVEL FILLINGS $1/2$ AND $1/4$

Figure S4(b) shows R_{xx} vs B traces measured with $I = 20$ nA at $T \simeq 55$ mK for sample A. The trace shows a broad, smooth minimum at $\nu = 1/2$, flanked by the Jain-sequence FQHSs of two-flux composite fermions (2 CFs) at $\nu = p/(2p \pm 1)$; $p = 1, 2, 3, \dots$, e.g., at $\nu = 1/3, 2/5, 3/7, \dots, 9/19$, and $\nu = 2/3, 3/5, 4/7, \dots, 9/17$. The trace at higher fields (blue) is rather featureless near $\nu = 1/4$, with Jain-sequence FQHSs of four-flux CFs (4 CFs) observed on the flanks at $\nu = p/(4p \pm 1)$. Figure S4(a) presents the second derivative of the data shown in Fig. S4(b). Sharp peaks in $d^2 R_{xx}/dB^2$ are observed flanking $\nu = 1/2$ and $\nu = 1/4$, e.g., at $\nu = 9/17, 9/19, 6/23$, and $5/21$, consistent with developing Jain-sequence FQHSs of 2 CFs and 4 CFs. At $\nu = 1/2$ and $\nu = 1/4$, $d^2 R_{xx}/dB^2$ is featureless and remains close to zero over a range of B , consistent with compressible CF Fermi sea ground states at $\nu = 1/2$ and $\nu = 1/4$ [1–4]. This is in stark contrast to the sharp peaks observed at odd-denominator Jain-sequence fillings and the even-denominator $\nu = 1/6$ [see Figs. S2(b) and S3(b)].

In Fig. S5, we present R_{xx} data for sample B. Qualitatively similar behaviors near $\nu = 1/2$ and $1/4$ are also observed in sample B. Compared to sample A, higher-order Jain-sequence FQHSs in sample B are observed on the flanks of $\nu = 1/2$ up to $\nu = 12/23$ and $12/25$, thanks to the lower sample temperature ($\simeq 40$ mK) and higher 2D electron density (7.1×10^{10} cm $^{-2}$). We note that sample B exhibits a weak, broad maximum at $\nu = 1/2$. The origin of this maximum is unclear. No R_{xx} minimum is observed at $\nu = 1/4$. $d^2 R_{xx}/dB^2$ is featureless and remains close to zero near $\nu = 1/2$ and $1/4$.

III. TEMPERATURE DEPENDENCE AND ACTIVATION ENERGY NEAR LANDAU LEVEL FILLING $1/6$

Figure S6(a) shows the high-field R_{xx} vs B traces taken at different temperatures ranging from 80 mK to 142 mK. In Fig. S6(b), we present activation energy (E_A) data, deduced from the relation $R_{xx} \propto e^{E_A/2kT}$, as a function of B . Figure S6(c) shows R_{xx} vs $1/T$ Arrhenius plots and the linear fits whose slopes give the value of E_A at a given B . The magnitude of E_A is associated with the defect formation energy of WC. Numerical calculations indicate

that, at high B , a WC formed by ${}^4\text{CFs}$ has lower energy than the conventional Hartree-Fock electron crystal [5], and that the lowest-energy *intrinsic* defect in this ${}^4\text{CF}$ WC is a hyper-correlated quantum bubble defect [6]. Recent measurements [7] on ultrahigh-quality two-dimensional electron systems (2DESs) similar to our sample, indeed exhibit E_A values which are in agreement with what is expected for an ideal ${}^4\text{CF}$ WC with no disorder, consistent with the fact that the WC domains in these samples are estimated to contain $\simeq 1000$ electrons [8].

Note that Fig. S6(b) data also reveal clear minima at $\nu = 1/7$, $2/11$, and $1/6$, where signatures of developing FQHSs are observed in the R_{xx} vs B data in Figs. S6(a). Similar minima in E_A were reported in modest-quality GaAs 2DESs at $\nu = 1/5$ [9] and very recently in ultrahigh-quality GaAs 2DESs at $\nu = 1/7$ [10], and were interpreted as precursors to developing FQHSs. The observation of an E_A minimum at $\nu = 1/6$ in Fig. S6(b) therefore supports the notion that the ground state at this filling is a FQHS.

IV. DATA FOR SAMPLES WITH DIFFERENT GaAs QUANTUM WELL WIDTHS

To investigate the role of quantum well (QW) width on the $1/6$ FQHS, we studied several samples with similar densities $n = 4.4, 4.3, 4.5$ and 4.3 (in units of 10^{10} cm^{-2}), but different QW widths of 70, 50, 40, and 30 nm, respectively; see Table I in the main text for sample parameters. In all the samples, we observe clear R_{xx} minima or inflection points at $\nu = 1/7, 2/13$, and $2/11$; see Figs. S6(a) and S7. They become more pronounced at lower temperatures, signaling the emergence of developing Jain-sequence FQHSs of ${}^6\text{CFs}$. These features attest to the exceptionally high quality of all the samples.

At $\nu = 1/6$, the FQHS feature becomes weaker in narrower QWs: In contrast to the clear R_{xx} minimum we observe in the 70-nm-wide sample, the 50 and 40-nm-wide samples exhibit a weak inflection point in R_{xx} [also evidenced by the sharp peak in d^2R_{xx}/dB^2 centered at $\nu = 1/6$; see Figs. S7(b, c)], while the 30-nm-wide sample is featureless near $\nu = 1/6$; see Fig. S7(d). In Fig. S7, we do not show data at lower T because the out-of-phase (capacitive) signal becomes comparable or even larger than the in-phase (resistive) signal and R_{xx} cannot be measured reliably near $\nu = 1/6$.

In Fig. S8, we present low- B traces for the three samples shown in Figs. S7(b-d). Qualitatively similar behaviors are observed in these samples: A smooth, shallow R_{xx} minimum

is seen at $\nu = 1/2$, while no R_{xx} minimum is observed at $\nu = 1/4$. These observations are consistent with what we see in Figs. S4 and S5 for the 70-nm-wide and the 58.5-nm-wide samples (samples A and B).

V. COMPARISON WITH PHASE DIAGRAMS FOR 1/2 FQHS IN WIDE GaAs QUANTUM WELLS

In order to contrast the relevant parameters of our samples with those which exhibit the $\nu = 1/2$ and $1/4$ FQHSs, we present Fig. S9. This figure contains “phase diagrams” for the stability of the $\nu = 1/2$ FQHS in wide GaAs QWs [11]. Figure S9(a) shows a plot of QW well width (w) vs density n , with the yellow-shaded area marking the parameter range where the $\nu = 1/2$ FQHS is stable, and the cyan and blue circles denoting where $\nu = 1/4$ FQHS has been reported [12, 13]. We have also included two data points (red stars) for the parameters of our samples A and B which exhibit clear minima at $\nu = 1/6$. In Fig. S9(b), we show the same phase diagrams and data, but now the axes are \tilde{w}/l_B and Δ_{SAS}/E_{Coul} .

VI. IMBALANCE DATA

In Fig. S10, we present R_{xx} vs $1/\nu$ traces for the 70-nm-wide QW at a fixed density of $4.6 \times 10^{10} \text{ cm}^{-2}$ with imbalanced charge distributions. (Front and back gates with opposite polarities were used to achieve these imbalanced charge distributions.) We observe R_{xx} minima at $\nu = 2/11$, $2/13$, and $1/7$. A clear inflection point is observed at $\nu = 1/6$ in all traces. Figure S11 shows ΔR_{xx} vs $1/\nu$ traces, revealing the evolution of FQHS features with imbalanced charge distributions more clearly. Sharp ΔR_{xx} minima are observed at $\nu = 2/11$, $3/17$, $2/13$, $1/7$, and $1/6$ in all traces. The FQHS features at odd-denominator fillings $\nu = 2/11$, $3/17$, $2/13$, and $1/7$ are rather insensitive to charge imbalance, consistent with what is expected for one-component, Jain-sequence FQHSs in a single-layer system. The FQHS feature at $\nu = 1/6$ is also robust against large charge asymmetry ($\Delta n/n \sim 50\%$), suggesting that the $\nu = 1/6$ FQHS we observe also has a one-component origin.

VII. HALL DATA

In Fig. S12, we present Hall slope (dR_H/dB) and Hall resistance (R_H) for sample A. We observe flat quantized Hall plateaus at integer fillings $\nu = 1, 2, \dots$ and fractional fillings, e.g., at $\nu = 1/3$ and $1/5$. Weaker Jain-sequence FQHSs that are not fully developed manifest themselves as developing plateaus in R_H and sharp minima in dR_H/dB , e.g., at $\nu = 6/11$ and $6/13$. Near $\nu = 1/2$ and $1/4$, R_H is linear and dR_H/dB is featureless, consistent with metallic Fermi seas of ${}^2\text{CF}$ and ${}^4\text{CF}$. It is worth noting that for $\nu < 1/5$ and $1/5 < \nu < 2/9$, R_H significantly deviates from the classical Hall line and dR_H/dB exhibits a complex behavior. This is because of the severe R_{xx} mixing into the R_H measurement when the 2DES enters a highly insulating regime where WC states prevail [14, 15], and because of the loss of Ohmic contact to the 2DES when R_{xx} becomes immeasurably large.

To reduce the mixing of R_{xx} and more accurately measure R_H at extremely small $\nu \sim 1/6$, we perform Hall measurements at elevated temperatures, where the ratio R_{xx}/R_H is smaller. Figure S13 shows R_H and dR_H/dB traces taken at two different temperatures. At $T \simeq 150$ mK, the Hall plateaus and the corresponding dR_H/dB minima at low B (e.g., at $\nu = 1, 1/3$, and $1/5$) are much weaker compared to the low temperature data shown in Fig. S12. Here, R_H begins to show mixing from R_{xx} and significantly deviates from the classical Hall line near $\nu \sim 1/6$. However, no features are observed in the range $1/5 > \nu > 1/6$. At $T \simeq 177$ mK, R_H follows the classical Hall line down to a lower filling ($\nu \sim 1/7$). Again, no features are observed in the range $1/5 > \nu > 1/7$.

It is important to note that Jain-sequence FQHSs of ${}^6\text{CFs}$ are much more fragile compared to those of ${}^2\text{CFs}$ and ${}^4\text{CFs}$. Theoretical studies report gap energies of approximately 0.1, 0.03, and 0.007 (in units of the Coulomb energy, $e^2/4\pi\epsilon\epsilon_0 l_B$) for the $\nu = 1/3, 1/5$, and $1/7$ FQHSs, respectively [16]. Consistent with this trend, in Fig. S13, the Hall plateau at $\nu = 1/5$ is indeed more fragile against increasing temperature than the $\nu = 1/3$ plateau. At even smaller fillings in the regime of ${}^6\text{CFs}$, the strength of the R_{xx} minimum at $\nu = 1/6$ is comparable to those at $\nu = 2/13$ and $3/17$ [see Fig. 1 of main text]. They get weaker rapidly and eventually disappear when T is increased from 80 mK to 142 mK [Fig. 1], in stark contrast to the $\nu = 1/5$ R_{xx} minimum which survives up to $T > 300$ mK. Therefore, the absence of Hall plateaus at $\nu = 1/6$ and Jain-sequence fillings $\nu = 1/7, 2/13, 3/19$, and $2/11, 3/17$ at elevated temperatures is not unexpected.

In Fig. S14, we present R_H data measured at intermediate temperatures, where R_{xx} minima or inflection points are observed at the even-denominator filling factor $\nu = 1/6$ and the odd-denominator filling factors $\nu = 1/7, 2/13, 3/17$, and $2/11$. At these temperatures, R_H exhibits a plateau quantized at $5h/e^2$ and a pronounced minimum in dR_H/dB developing at $\nu = 1/5$. At higher B , significant deviations of R_H from the classical Hall resistance B/ne , caused by the mixing of R_{xx} , are clearly visible. The magnitudes of these deviations show sharp minima at $\nu = 1/7, 2/13, 3/17, 2/11$, and $\nu = 1/6$, which qualitatively mirror the R_{xx} data observed at similar temperatures. We also note that, as we increase the temperature, these sharp minima weaken and disappear before the mixing of R_{xx} is eliminated.

To conclude, there are two factors that prevent us from measuring quantized Hall plateaus at extremely small ν : (i) At low temperatures, Hall resistance cannot be measured reliably because of the severe R_{xx} mixing effect caused by the dominant insulating phase. (ii) At higher temperatures, the fragile FQHSs at extremely small fillings (e.g., at $\nu = 1/7, 2/11$ and $1/6$) diminish in strength and eventually vanish. Unfortunately, there is no temperature range within which we can reliably measure Hall resistance while the FQHSs at small ν still survive.

-
- [1] R. L. Willett, R. R. Ruel, K. W. West, and L. N. Pfeiffer, Experimental demonstration of a Fermi surface at one-half filling of the lowest Landau level, *Phys. Rev. Lett.* **71**, 3846 (1993).
 - [2] W. Kang, H. L. Stormer, L. N. Pfeiffer, K. W. Baldwin, and K. W. West, How real are composite fermions?, *Phys. Rev. Lett.* **71**, 3850 (1993).
 - [3] D. Kamburov, Yang Liu, M. A. Mueed, M. Shayegan, L. N. Pfeiffer, K. W. West, and K. W. Baldwin, What Determines the Fermi Wave Vector of Composite Fermions?, *Phys. Rev. Lett.* **113**, 196801 (2014).
 - [4] Md. Shafayat Hossain, Meng K. Ma, M. A. Mueed, D. Kamburov, L. N. Pfeiffer, K. W. West, K. W. Baldwin, R. Winkler, and M. Shayegan, Geometric resonance of four-flux composite fermions, *Phy. Rev. B* **100**, 041112(R) (2019).
 - [5] Alexander C. Archer, Kwon Park, and Jainendra K. Jain, Competing Crystal Phases in the Lowest Landau Level, *Phys. Rev. Lett.* **111**, 146804 (2013).
 - [6] Alexander C. Archer and Jainendra K. Jain, Quantum bubble defects in the lowest-Landau-

- level crystal, Phys. Rev. B **90**, 201309 (2014).
- [7] P. T. Madathil, C. Wang, S. K. Singh, A. Gupta, K. A. Villegas Rosales, Y. J. Chung, K. W. West, K. W. Baldwin, L. N. Pfeiffer, L. W. Engel, and M. Shayegan, Signatures of Correlated Defects in an Ultraclean Wigner Crystal in the Extreme Quantum Limit, Phys. Rev. Lett. **132**, 096502 (2024).
- [8] P. T. Madathil, K. A. Villegas Rosales, Y. J. Chung, K. W. West, K. W. Baldwin, L. N. Pfeiffer, L. W. Engel, and M. Shayegan, Moving Crystal Phases of a Quantum Wigner Solid in an Ultra-High-Quality 2D Electron System, Phys. Rev. Lett. **131**, 236501 (2023).
- [9] R. L. Willett, H. L. Stormer, D. C. Tsui, L. N. Pfeiffer, K. W. West, and K. W. Baldwin, Termination of the series of fractional quantum Hall states at small filling factors, Phys. Rev. B **38**, 7881(R) (1988).
- [10] Yoon Jang Chung, D. Graf, L. W. Engel, K. A. Villegas Rosales, P. T. Madathil, K. W. Baldwin, K. W. West, L. N. Pfeiffer, and M. Shayegan, Correlated States of 2D Electrons near the Landau Level Filling $\nu = 1/7$, Phys. Rev. Lett. **128**, 026802 (2022).
- [11] J. Shabani, Yang Liu, M. Shayegan, L. N. Pfeiffer, K. W. West, and K. W. Baldwin, Phase diagrams for the stability of the $\nu = 1/2$ fractional quantum Hall effect in electron systems confined to symmetric, wide GaAs quantum wells, Phys. Rev. B **88**, 245413 (2013).
- [12] D. R. Luhman, W. Pan, D. C. Tsui, L. N. Pfeiffer, K. W. Baldwin, and K. W. West, Observation of a Fractional Quantum Hall State at $\nu = 1/4$ in a Wide GaAs Quantum Well, Phys. Rev. Lett. **101**, 266804 (2008).
- [13] J. Shabani, T. Gokmen, and M. Shayegan, Correlated States of Electrons in Wide Quantum Wells at Low Fillings: The Role of Charge Distribution Symmetry, Phys. Rev. Lett. **103**, 046805 (2009).
- [14] V. J. Goldman, J. K. Wang, B. Su, and M. Shayegan, Universality of the Hall effect in a magnetic-field-localized two-dimensional electron system, Phys. Rev. Lett. **70**, 647 (1993).
- [15] T. Sajoto, Y. P. Li, L. W. Engel, D. C. Tsui, and M. Shayegan, Hall resistance of the reentrant insulating phase around the $1/5$ fractional quantum Hall liquid, Phys. Rev. Lett. **70**, 2321 (1993).
- [16] Zheng-Wei Zuo, Ajit C. Balram, Songyang Pu, Jianyun Zhao, Thierry Jolicoeur, A. Wójs, and J. K. Jain, Interplay between fractional quantum Hall liquid and crystal phases at low filling, Phys. Rev. B **102**, 075307 (2020).

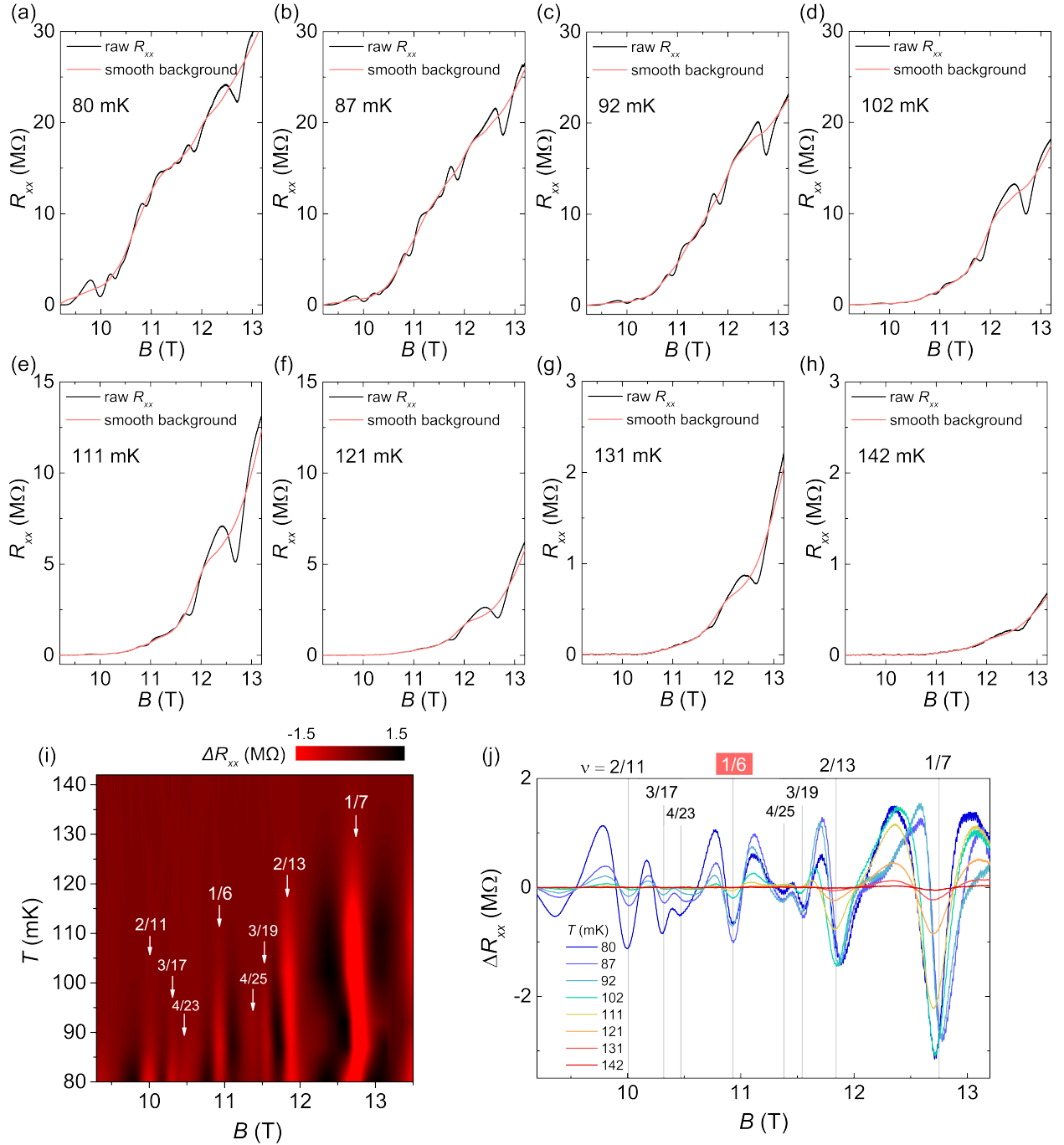


Fig. S1. **Extracting FQHS features from R_{xx} with an increasing resistance background.** (a-h) R_{xx} vs B traces (black) and resistance background (red) obtained using Savitzky–Golay smoothing. (i) Color-scale plot of ΔR_{xx} as a function of B and T , where ΔR_{xx} is the resistance after subtracting the increasing background. (j) ΔR_{xx} vs B traces at different T .

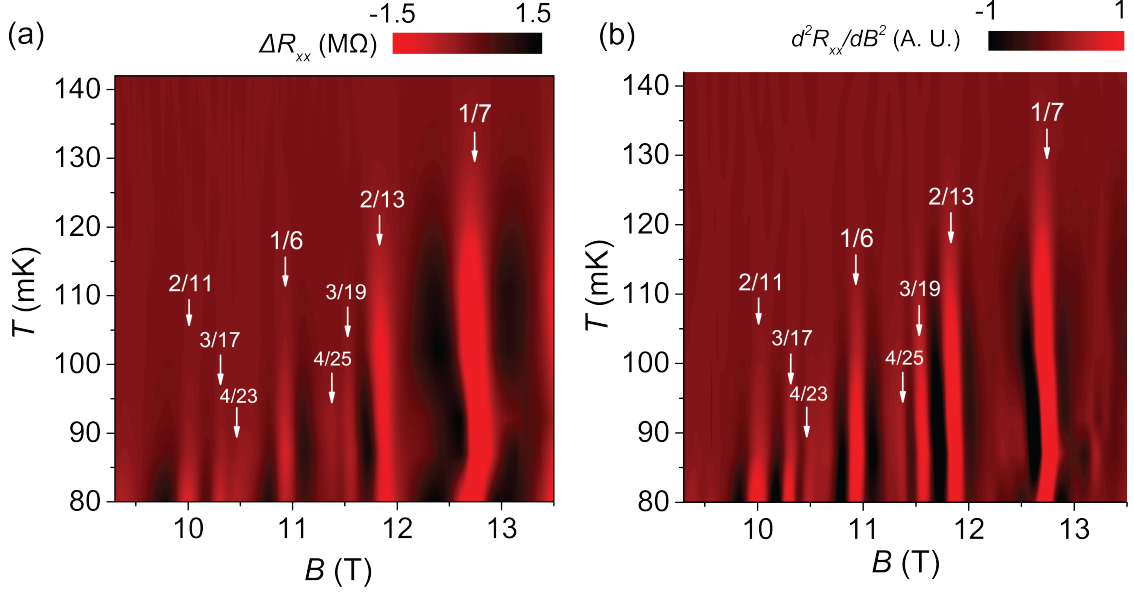


Fig. S2. **Comparison between ΔR_{xx} and $d^2 R_{xx}/dB^2$ data.** (a) Color-scale plot of ΔR_{xx} as a function of B and T , adapted from Fig. S1(i). (b) Color-scale plot of $d^2 R_{xx}/dB^2$ as a function of B and T .

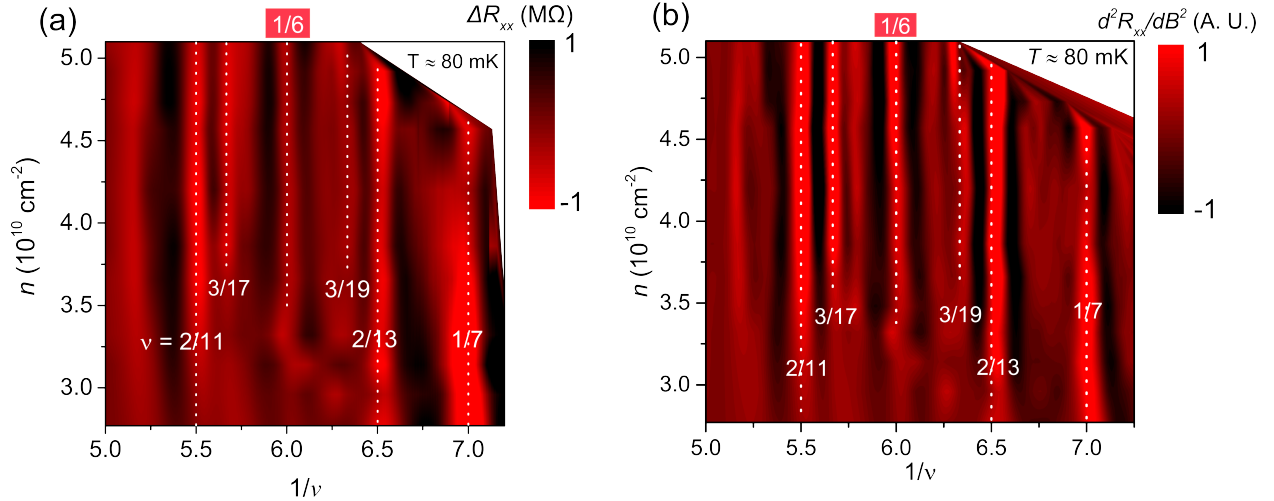


Fig. S3. **Comparison between ΔR_{xx} and $d^2 R_{xx}/dB^2$ data.** (a) Color-scale plot of ΔR_{xx} as a function of $1/\nu$ and n , adapted from Fig. 2(b) of the main text. (b) Color-scale plot of $d^2 R_{xx}/dB^2$ as a function of $1/\nu$ and n .

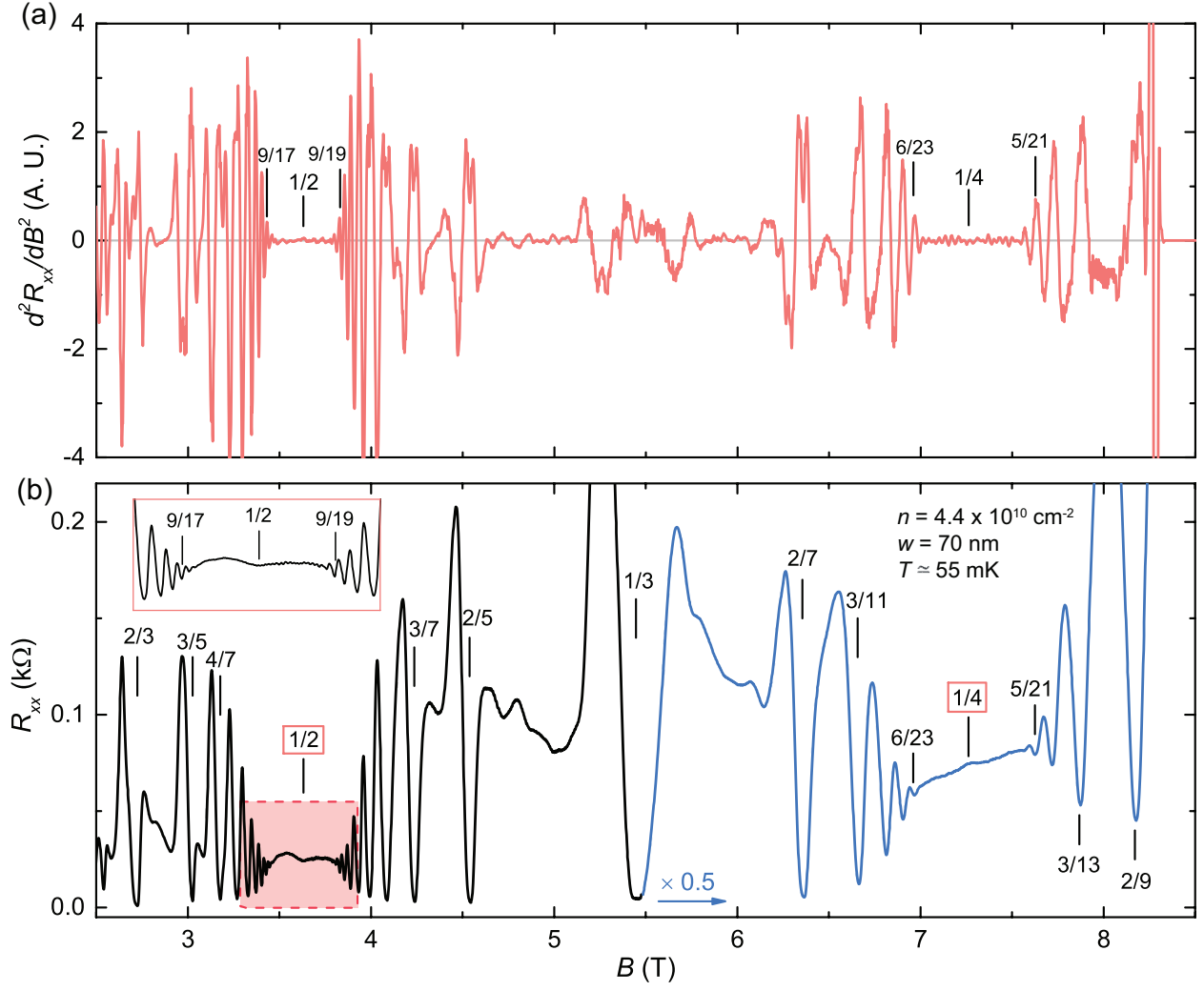


Fig. S4. **Magnetoconductance near $\nu = 1/2$ and $1/4$ for sample A.** (a) d^2R_{xx}/dB^2 and (b) R_{xx} vs B traces measured with $I = 20 \text{ nA}$ at $T \approx 55 \text{ mK}$. In (b), the magnitude of the trace for $B > 5.5 \text{ T}$ is multiplied by 0.5.

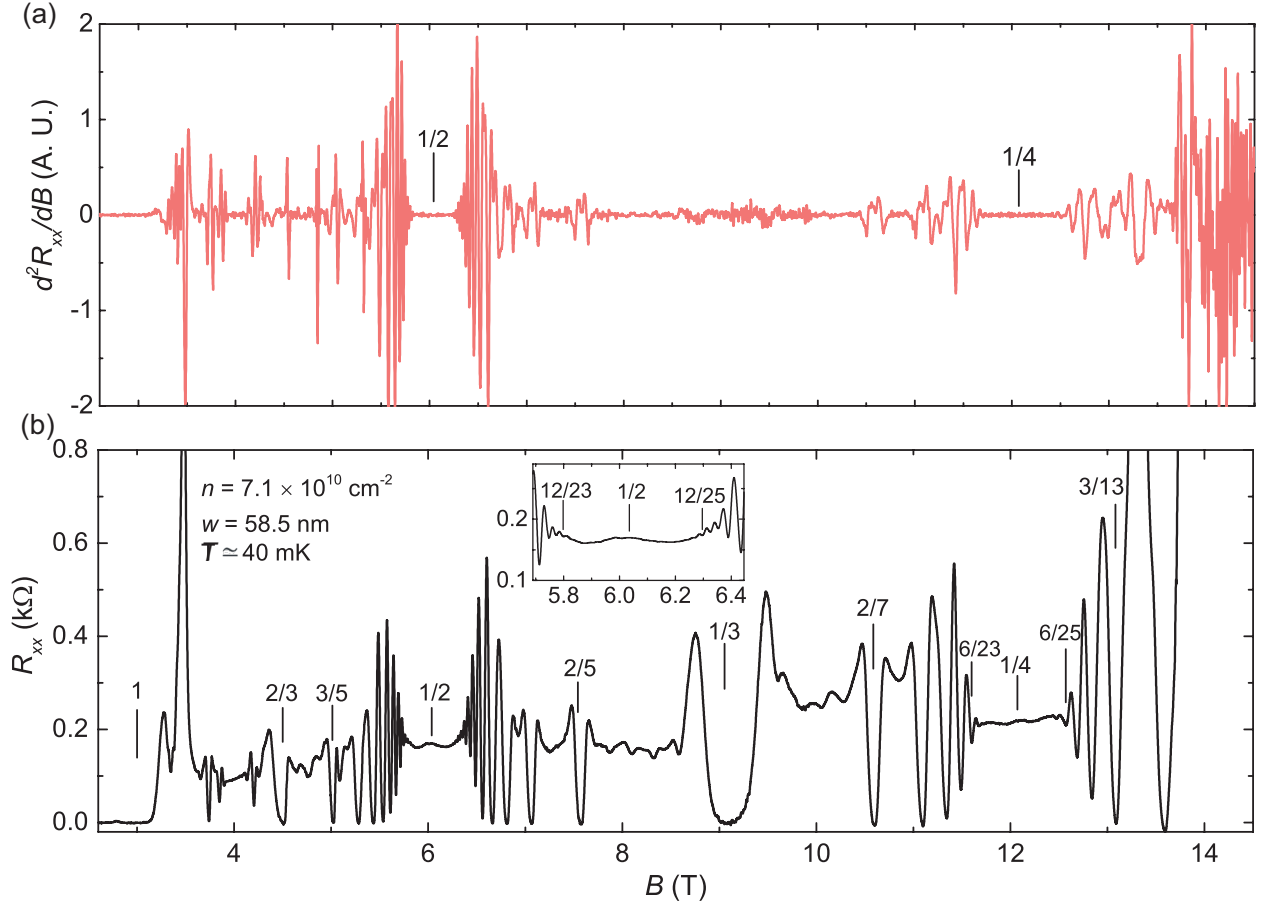


Fig. S5. **Magnetoconductance near $\nu = 1/2$ and $1/4$ for sample B.** (a) d^2R_{xx}/dB^2 and (b) R_{xx} vs B traces measured with $I = 20 \text{ nA}$ at $T \approx 40 \text{ mK}$.

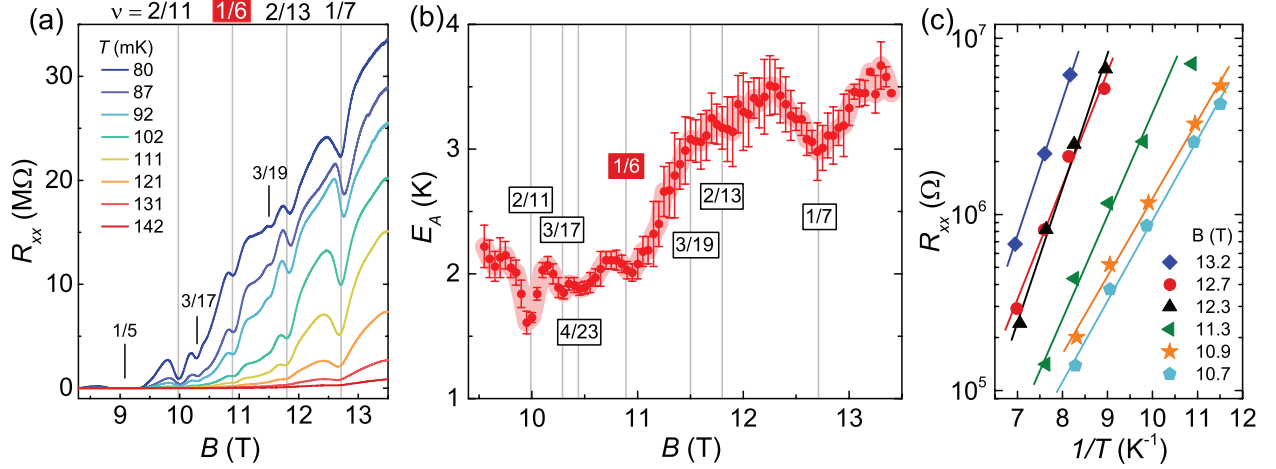


Fig. S6. **Temperature dependence and activation energy.** (a) R_{xx} vs B traces taken during up sweeps of B at different temperatures. Several Landau level fillings are marked. (b) Activation energy E_A deduced from the relation $R_{xx} \propto e^{E_A/2kT}$. (c) R_{xx} vs $1/T$ Arrhenius plots at various B . The solid lines show linear fits whose slopes give the value of E_A .

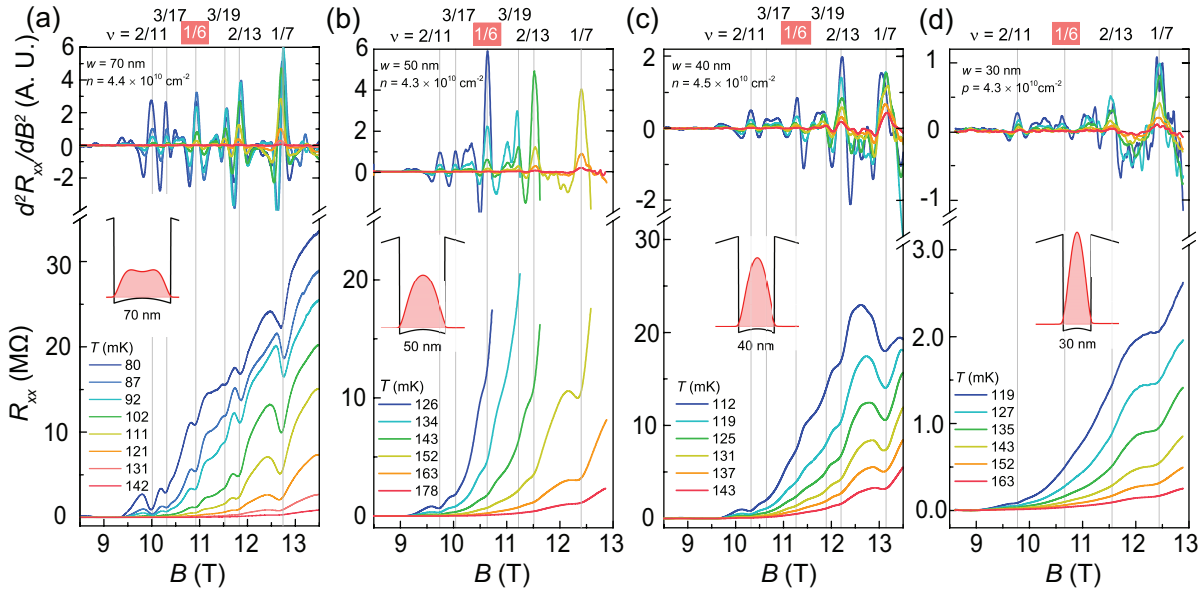


Fig. S7. **Data near $\nu = 1/6$ for samples with different GaAs QW widths.** R_{xx} and $d^2 R_{xx} / dB^2$ vs B traces taken at different temperatures for: (a) $w = 70$ nm, $n = 4.4$; (b) $w = 50$ nm, $n = 4.3$; (c) $w = 40$ nm, $n = 4.5$; (d) $w = 30$ nm, $n = 4.3$. Insets: Self-consistent charge distributions (red) and potentials (black) for 2DESs confined to QWs with different widths.

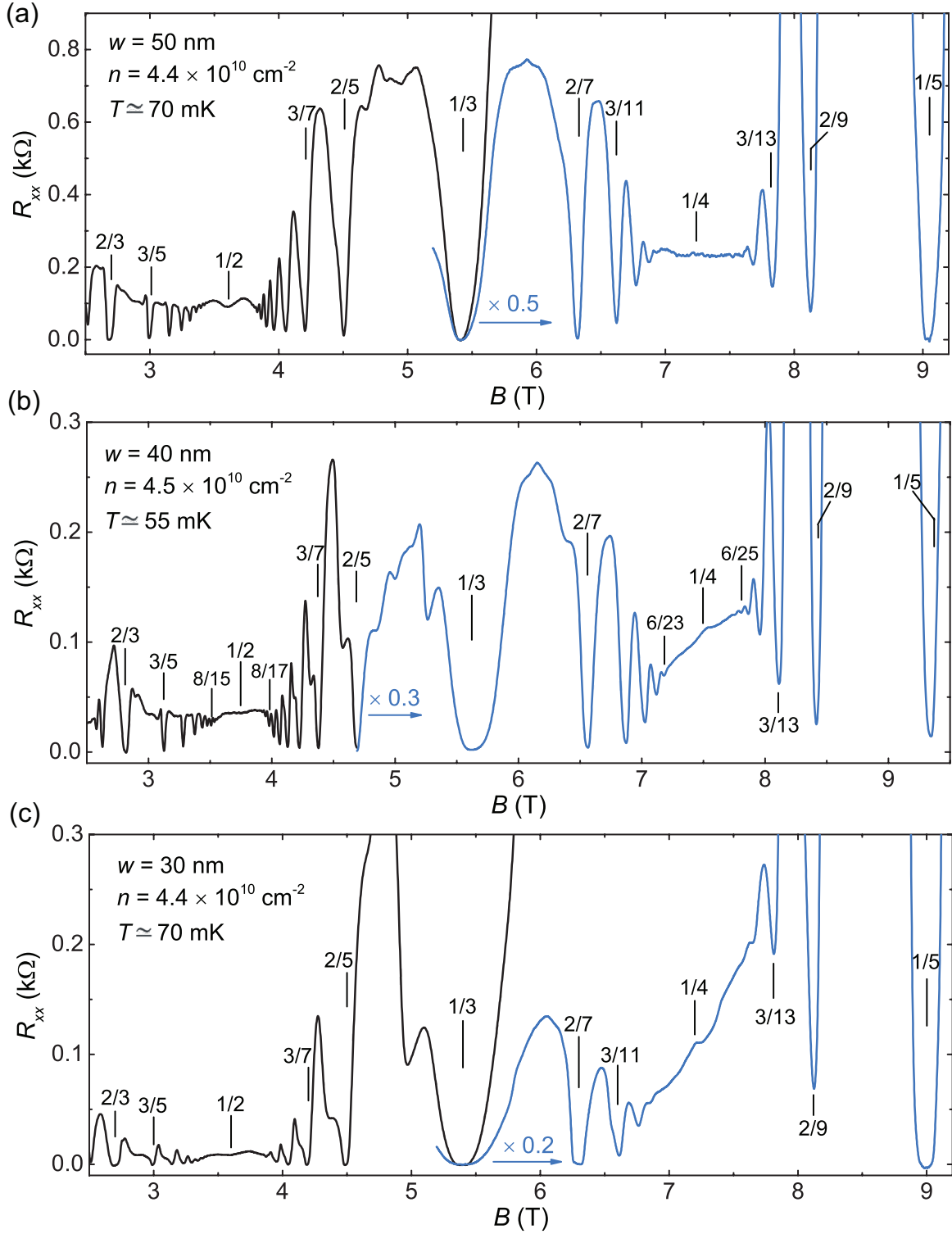


Fig. S8. Data near $\nu = 1/2$ and $\nu = 1/4$ for samples with different GaAs QW widths. R_{xx} vs B traces for three different samples: (a) $w = 50$ nm, $n = 4.3$; (b) $w = 40$ nm, $n = 4.5$; (c) $w = 30$ nm, $n = 4.3$.

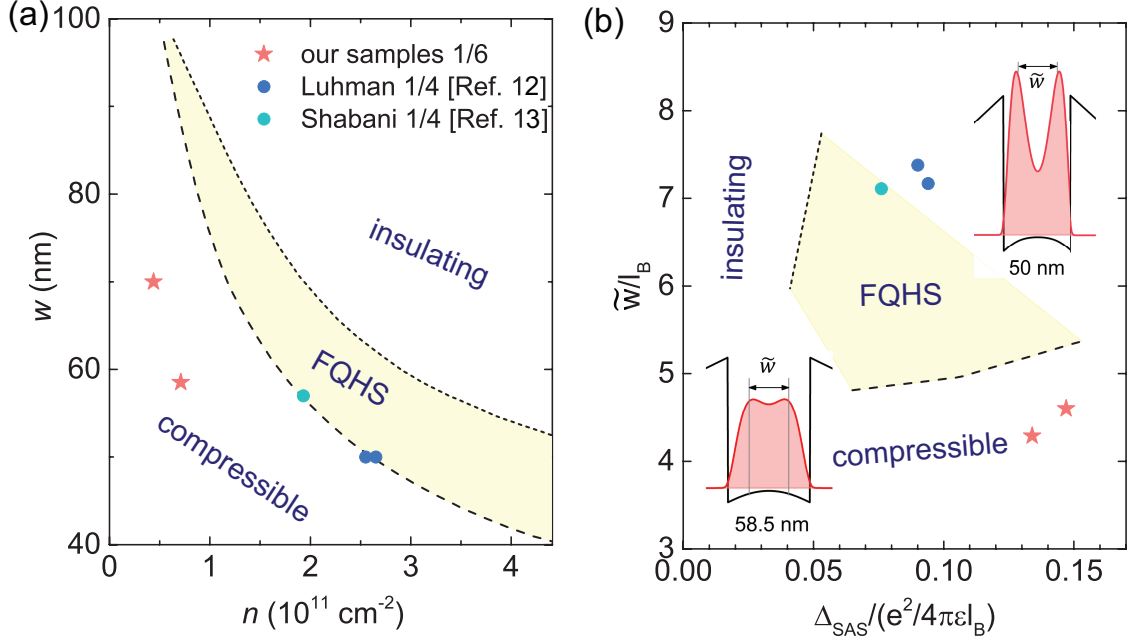


Fig. S9. **Comparison with phase diagrams for 1/2 FQHS in wide GaAs QWs.** (a) w vs n , and (b) \tilde{w}/l_B vs $\Delta_{SAS}/(e^2/4\pi\epsilon|_B)$ phase diagrams showing the region, marked in yellow, in which the 1/2 FQHS is stabilized. As described in the main text, \tilde{w} is the effective electron layer thickness, defined as twice the standard deviation of the charge distribution from its center; see the charge distributions in (b). The dashed and dotted lines are experimental phase boundaries adopted from Ref. [11]. The cyan and blue circles mark the points where a 1/4 FQHS was reported [12, 13]. These points fall in the region where the 1/2 FQHS is stabilized. The two red stars mark the points where we observe strong FQHS features at $\nu = 1/6$ (samples A and B in Table. I). Both points fall well outside the yellow region in both phase diagrams. Insets in (b) show self-consistent charge distributions (red) and potentials (black) for two samples: $n = 7.1, w = 58.5 \text{ nm}$ (bottom-left) where we observe a developing 1/6 FQHS, and $n = 26.5, w = 50 \text{ nm}$ (top-right) where a 1/4 FQHS has been reported in Ref. [12].

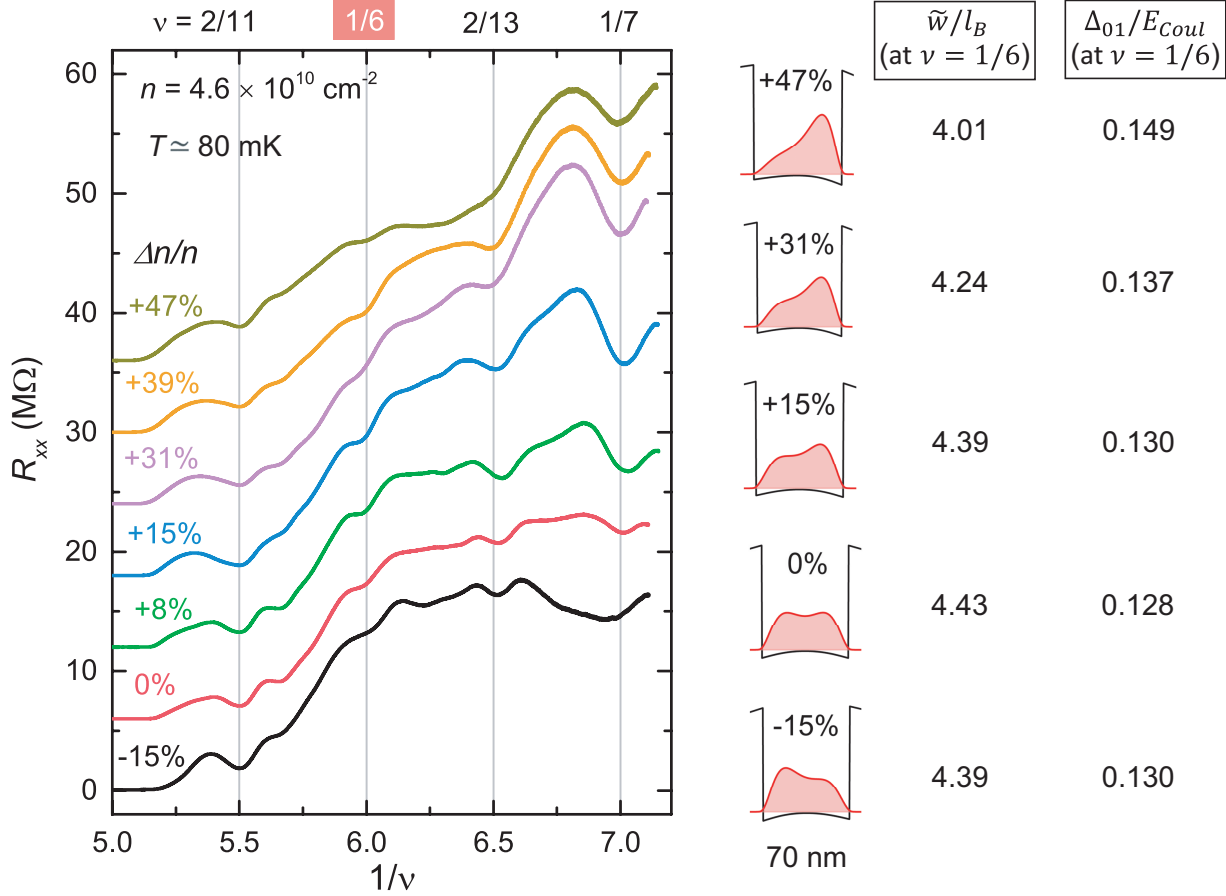


Fig. S10. **Imbalance data.** R_{xx} vs $1/\nu$ traces for the 70-nm-wide GaAs QW at a fixed density of $4.6 \times 10^{10} \text{ cm}^{-2}$ with imbalanced charge distributions. Each trace is vertically shifted by $2 \text{ M}\Omega$ for clarity. Self-consistent charge distributions (red) and potential (black) for typical $\Delta n/n$ values are shown on the right. Δn is defined as twice the density transferred from one side of the QW to the other. Also listed are \tilde{w}/l_B and Δ_{01}/E_{Coul} , where Δ_{01} is the energy difference between the ground-state and excited-state electric subbands. For the case where the charge distribution is symmetric ($\Delta n/n = 0$), $\Delta_{01} = \Delta_{SAS}$.

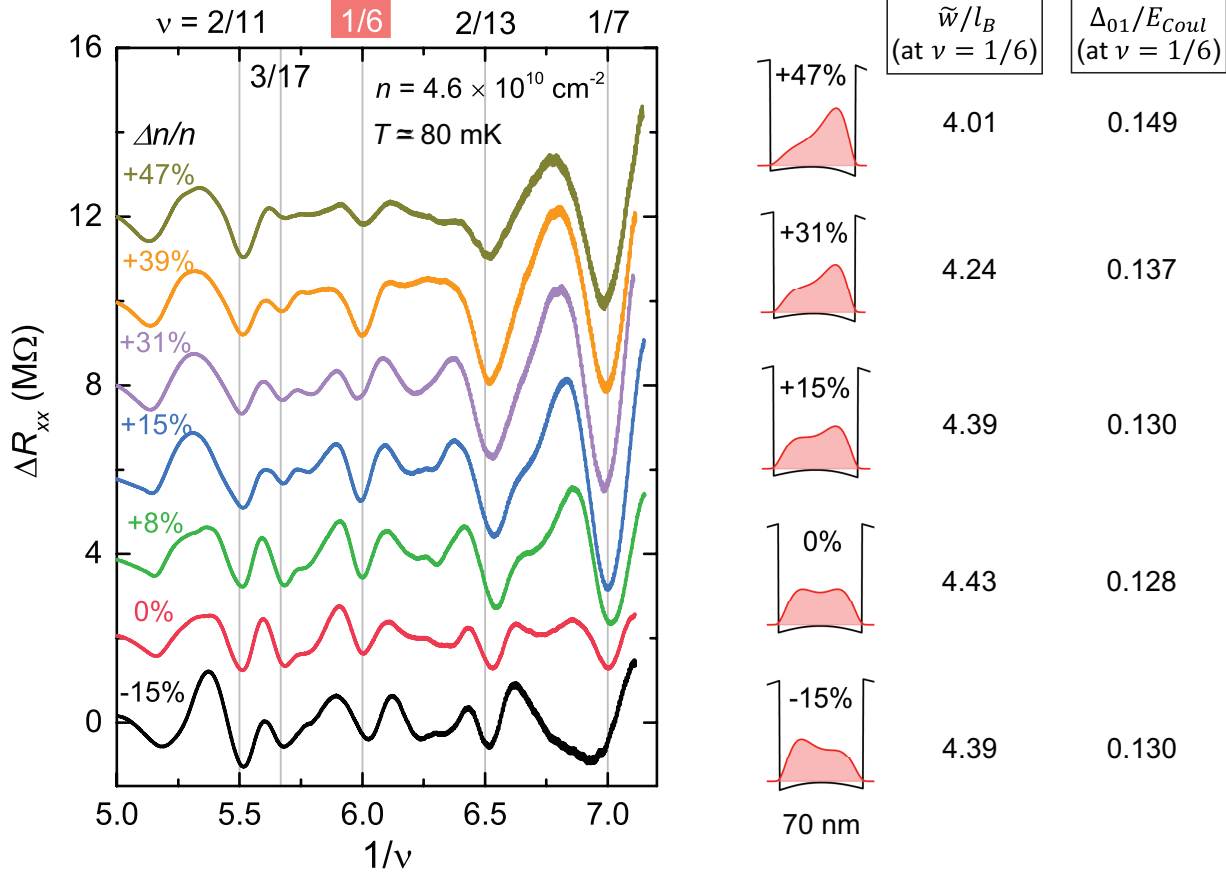


Fig. S11. **Imbalance data after subtracting smooth background.** ΔR_{xx} vs $1/\nu$ traces for the 70-nm-wide GaAs QW at a fixed density of $4.6 \times 10^{10} \text{ cm}^{-2}$ with imbalanced charge distributions. Each trace is vertically shifted by $2 \text{ M}\Omega$ for clarity. Self-consistent charge distributions (red) and potential (black) for typical $\Delta n/n$ values are shown on the right. Δn is defined as twice the density transferred from one side of the QW to the other. Also listed are \tilde{w}/l_B and Δ_{01}/E_{Coul} , where Δ_{01} is the energy difference between the ground-state and excited-state electric subbands. For the case where the charge distribution is symmetric ($\Delta n/n = 0$), $\Delta_{01} = \Delta_{SAS}$.

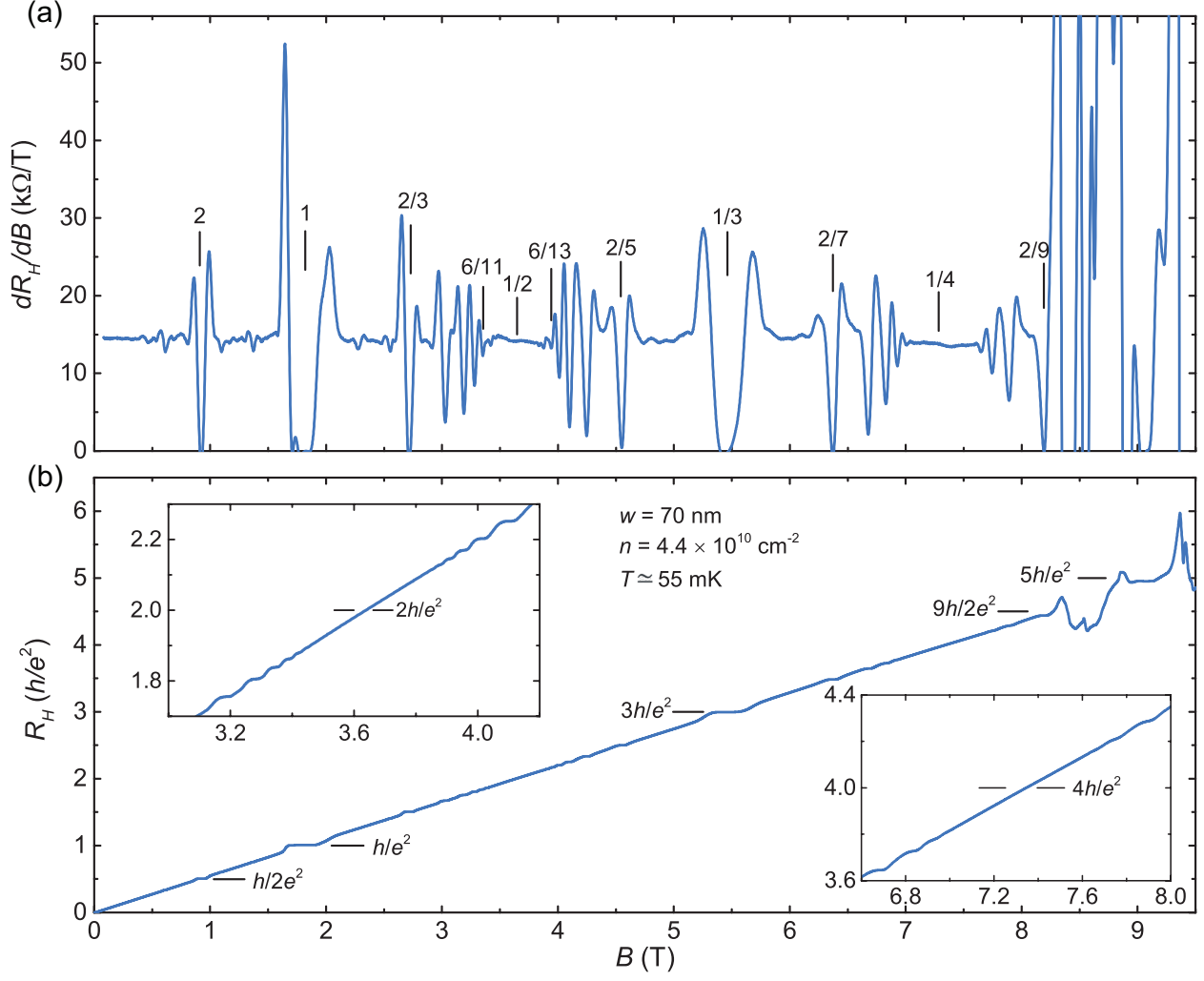


Fig. S12. **Hall data near $\nu = 1/2$ and $1/4$.** (a) Hall slope dR_H/dB and (b) Hall resistance R_H vs B traces for sample A measured at $T \simeq 55$ mK. Insets in (b) present the enlarged version of R_H vs B data near $\nu = 1/2$ and $1/4$.

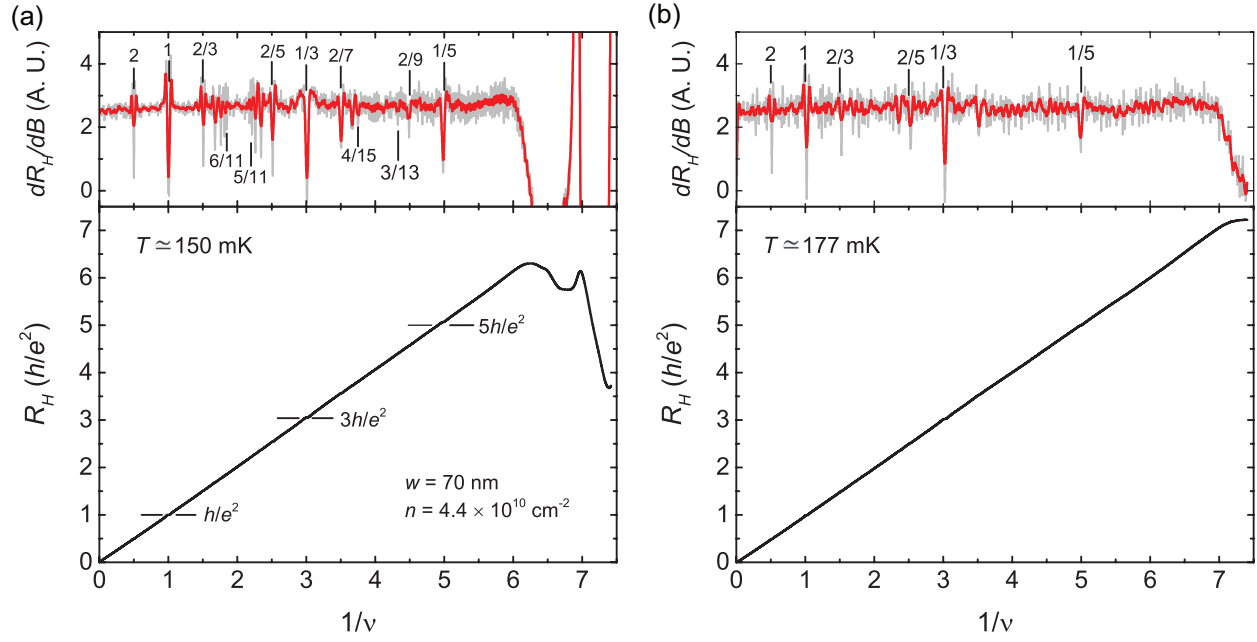


Fig. S13. **Full-field Hall data at elevated temperatures.** dR_H/dB (top panels) and R_H (bottom panels) vs B traces for sample A measured at (a) $T \simeq 150$ mK and (b) $T \simeq 177$ mK.

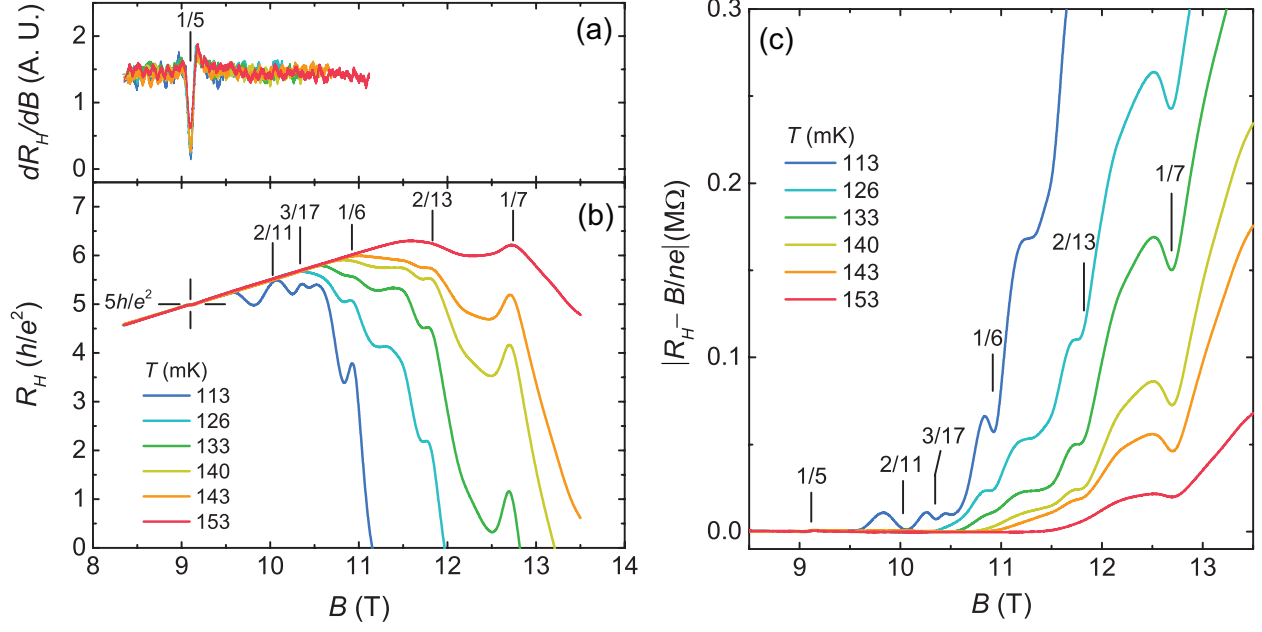


Fig. S14. **High-field Hall data at different temperatures.** (a) dR_H/dB and (b) R_H vs B traces for sample A measured at different temperatures ranging from $T \simeq 113$ mK to $T \simeq 153$ mK. Significant R_{xx} mixing effect is observed at high $B > 9$ T (low $\nu < 1/5$). (c) Deviation of measured R_H from the classical Hall value B/ne .